Pontifícia Universidade Católica
do Rio de Janeiro

**Lhaylla dos Santos Crissaff**

# Geometric Energies on Triangulated Surfaces



**TESE DE DOUTORADO**

Thesis presented to the Postgraduate Program in Mathematics of the Departamento de Matemática, PUC–Rio as partial fulfillment of the requirements for the degree of Doutor em Matemática

Advisor : Prof. Marcos Craizer
Co–Advisor: Prof. Sinésio Pesco

Rio de Janeiro
February 2009

Pontifícia Universidade Católica
do Rio de Janeiro

**Lhaylla dos Santos Crissaff**

# Geometric Energies on Triangulated Surfaces

**Thesis presented to the Postgraduate Program in Mathematics, of the Departamento de Matemática do Centro Técnico Científico da PUC–Rio, as partial fulfillment of the requirements for the degree of Doutor.**

**Prof. Marcos Craizer**
Advisor
Departamento de Matemática — PUC–Rio

**Prof. Sinésio Pesco**
Co–Advisor
Departamento de Matemática — PUC–Rio

**Prof. Ralph Costa Teixeira**
Universidade Federal Fluminense — UFF

**Prof. Luiz Henrique de Figueiredo**
Instituto Nacional de Matemática Pura e Aplicada — IMPA

**Prof. Moacyr Alvim Horta Barbosa da Silva**
Fundação Getulio Vargas — FGV

**Prof. Geovan Tavares dos Santos**
Departamento de Matemática — PUC–Rio

**Prof. Hélio Côrtes Vieira Lopes**
Departamento de Matemática — PUC–Rio

**Prof. Thomas Lewiner**
Departamento de Matemática — PUC–Rio

**Prof. José Eugênio Leal**
Coordinator of the Centro Técnico Científico da PUC–Rio

PUC–Rio Rio de Janeiro, — February 17, 2009

**Lhaylla dos Santos Crissaff**

Graduated in Mathematics from Universidade Federal Fluminense – UFF in 2003, she obtained the Master degree at PUC–Rio in Algebraic Geometry in 2005.



Bibliographic data

Crissaff, Lhaylla dos Santos

Geometric Energies on Triangulated Surfaces / Lhaylla dos Santos Crissaff; advisor: Marcos Craizer; co–advisor: Sinésio Pesco. — 2009.

v., 79 f: il. ; 29,7 cm

1. Tese(Doutorado em Matemática) - Pontifícia Universidade Católica do Rio de Janeiro, Rio de Janeiro, 2009.

Inclui bibliografia.

1. Matemática – Teses. 2. Área Discreta. 3. Superfície Mínima Discreta. 4. Laplaciano Discreto. 5. Energia Geométrica Discreta. I. Craizer, Marcos. II. Pesco, Sinésio. III. Pontifícia Universidade Católica do Rio de Janeiro. Departmento de Matemática. IV. Título.

CDD: 510

To my grandmother Maria (*in memoriam*).

## Acknowledgments

First of all, to God for all blessings granted me, that many people call luck or coincidence.

To my advisors Professors Marcos Craizer and Sinésio Pesco for the support to the realization of this work.

To my mother Leticia, who never had a chance to have an academic career. You will always be my mother, my father, my support, my best example, my breath... I am eternally gratefull to you.

To my sister Lhayzza, for her continual love and countless encouragement. I thank you for believing in me and helping me to realize my dream.

To my love Marcos Lage, who the enthusiasm for life allows me to look at the simplest of things with a sense of wonder. Only with your support, faith and unconditional love have I been able to complete this thesis.

To my grandmother, uncles, cousins, that understood my absence. In particular to my godmother Solange, who called me every week since I have left my city to study in Rio de Janeiro.

To my new family: Marcos, Lúcia and Cynthia, who opened the door of their house to me and shared all happiness and disappointments with me.

To all my professors during these last 10 years, among them Geovan Tavares and Thomas Lewiner. In special to Professor Hélio Lopes, who took a special interest in my progress and shared with me his vast professional and personal wisdom.

To all my friends and colleagues at the Department of Mathematics: João, Alex, Thales, Jéssica, Débora, Afonso among others, for providing a nice and friendly atmosphere. And in particular, to Fabiano for great companionship to gossip.

To Professor Konrad Polthier (FU Berlin), who gave me the opportunity of trying to understand mathematics in the other side of the world.

To people of the Mathematics department for the constant help: Creuza, Kátia, Otávio and Orlando.

To Faperj and PUC–Rio, for the financial support.

## Abstract

Crissaff, Lhaylla dos Santos; Craizer, Marcos; Pesco, Sinésio. **Geometric Energies on Triangulated Surfaces**. Rio de Janeiro, 2009. 79p. PhD Thesis — Department of Matemática, Pontifícia Universidade Católica do Rio de Janeiro.

In Computer Graphics, it is common to minimize energies defined on discrete objects to obtain models with desired properties. In this thesis, we consider energies defined on triangulated surfaces, invariant under rigid motions, that we have called geometric energies. First, we have studied discrete minimal triangulated surfaces, defined as critical points of the area functional. We have also proposed a new example of energy given by the sum of squares of the circumscribed radius of the triangles, that has presented nice results in terms of smoothing and good quality of the triangulation. Then we have looked for general properties of these energies, in particular the relation with discrete Laplacians. Our main result states that any discrete Laplacian coming from a geometric energy is symmetric and establish conditions for a symmetric Laplacian to come from a geometric energy. We have also studied the Willmore energy and proposed an alternative for its discrete version.



## Keywords

Discrete Area. Discrete Minimal Surface. Discrete Laplacian. Discrete Geometric Energy.

# Resumo

Crissaff, Lhaylla dos Santos; Craizer, Marcos; Pesco, Sinésio. **Energias Geométricas para superfícies trianguladas**. Rio de Janeiro, 2009. 79p. Tese de Doutorado — Departamento de Matemática, Pontifícia Universidade Católica do Rio de Janeiro.

Em computação gráfica é comum minimizar energias definidas sobre objetos discretos para obter modelos com propriedades desejadas. Nesta tese, consideramos energias definidas sobre superfícies trianguladas, invariantes por movimentos rígidos, chamadas energias geométricas. Primeiramente, estudamos superfícies mínimas discretas trianguladas, definidas como ponto crítico do funcional área. Também propusemos um novo exemplo de energia dada pela soma dos quadrados dos raios dos círculos circunscritos aos triângulos, que tem apresentado bons resultados em termos de suavidade e boa qualidade da triangulação. Então procuramos propriedades gerais destas energias, em particular a relação com Laplacianos discretos. Nosso principal resultado estabelece que todo Laplaciano discreto proveniente de uma energia geométrica é simétrico e estabelecemos condições para um Laplaciano simétrico ser proveniente de uma energia geométrica. Nós ainda estudamos a energia de Willmore e propusemos uma alternativa para sua versão discreta.



## Palavras–chave

Área Discreta. Superfície Mínima Discreta. Laplaciano Discreto. Energia Geométrica Discreta.

# Contents

# List of Figures

*"Não entendo. Isso é tão vasto que ultrapassa qualquer entender. Entender é sempre limitado. Mas não entender pode não ter fronteiras. Sinto que sou muito mais completa quando não entendo. Não entender, do modo como falo, é um dom. Não entender, mas não como um simples de espírito. O bom é ser inteligente e não entender. É uma benção estranha, como ter loucura sem ser doida. É um desinteresse manso, é uma doçura de burrice. Só que de vez em quando vem a inquietação: quero entender um pouco. Não demais: mas pelo menos entender que não entendo."*

**Clarice Lispector**, *A descoberta do mundo*.

# 1
# Introduction

In many research fields and, in particular, in Computer Graphics, it is common to minimize functions defined on triangulated surfaces. Such a minimization leads to new triangulated surfaces satisfying certain desired properties. In (28), for example, minimization of an energy is used to approximate the geometry of the vertices, given the connectivity of the mesh and the geometry of some selected vertices. In that paper, the energy minimization implies that an unknown vertex will be positioned in the center of gravity of its immediate neighbors. In (8), the same problem is considered, but a generalized energy is used to solve it. In (14), the minimization of a certain energy is used to provide the geometry of the entire mesh, given the connectivity. These are examples of problems formulated as global minimization of an energy.

There exist some known smooth functionals that were discretized and their discrete versions were used to solve problems analogous to the smooth case. Minimization of the *Dirichlet energy* solves the classic Plateau's problem, i.e., find a surface of minimum area with a given boundary curve. Such a surface is called a *minimal surface*. The problem is known since the Belgian physicist J.A. Plateau performed an extensive series of experiments using metal wire to represent curves and soap films to model minimal surfaces in the nineteenth century. In (21, 22) we find discrete analogous definitions of the Dirichlet energy and minimal surface. These papers work with a discrete version of the Plateau's problem and solution is called a *discrete minimal surface*. The notion of discrete minimal surface is not uniquely defined, since the various properties which characterize smooth minimal surfaces can be discretized in different ways. In (21, 22), the area of the triangulated surfaces is minimized, allowing also the constructing of a discrete analogous to conjugate minimal surfaces. On the other hand, in (3), Bobenko et al. presented a quadrangular discretization of minimal surfaces based on isothermal parameterizations.

Another known functional is the Willmore energy. The Willmore energy is a quantitative measure of how much a given surface deviates from a round sphere. A minimum of the Willmore energy is called *Willmore surface*. This functional is very important in conformal geometry, since it is conformally invariant. Numerically,

there are many approaches to find *discrete Willmore surfaces*, among them the one introduced by Bobenko in (1). It is worthwhile to mention that this discrete version approximates the smooth Willmore energy, when the triangulation is close to a smooth surface.

In this thesis, our main goal is to study discrete energies defined on triangulated surfaces that are invariant under rigid motions. These energies will be called *geometric energies*. Geometric energies can satisfy other properties such as *local support*, when the energy of a single triangle depends only on the geometry of the triangle and not on the neighbors triangles, and *additivity*, when the total energy is the sum of the geometric energies of the triangles.

An example of additive locally supported geometric energy is the *squared edges energy* described in Subsection 4.1.2. This energy is defined as the sum of squared edge lengths of the triangulated surface, which implies that a minimum of squared edges energy has all vertices in the center of gravity of its immediate neighbors. This energy is used in many works to smooth discrete surfaces and its gradient is called the *combinatorial Laplacian*.

Another important example of additive locally supported geometric energy is the area functional, described in Chapter 3. The discrete area of the triangulated surface is the sum of the area of all triangles of the surface. The gradient of the area is commonly called the *Laplacian of the cotangents* and it is very useful (see (21, 22, 23)).

We introduce a new example of additive locally supported geometric energy in Subsection 4.1.3 called *circumscribed radius energy*. This energy is defined as the sum of the squared radius of the circumscribed circles of all triangles in the surface. We have tested many examples with this energy and we observed that triangles obtained were far from degenerate and the surfaces were quite smooth.

In Chapter 4 we suggest a theoretical framework for analyzing additive locally supported geometric energies. It is easy to see that any such energy can be written as

$$E(M) = \sum_{T \in M} f(l_1, l_2, l_3)$$

where $M$ is a triangulated surface formed by triangles $T$ with sides $l_1, l_2, l_3$. The gradient of $E$ defines a discrete Laplacian. One of our main contribution is to characterize those discrete Laplacians that come from an additive locally supported geometric energy. We show that any discrete Laplacian that comes from a geometric energy is symmetric. Moreover, we establish a necessary and sufficient condition for a symmetric discrete Laplacian to come from a geometric energy. This condition is given in terms of the weights of a pair of adjacent edges and the angles of the

triangle determined by their. We also generalize the definition of the index of a discrete minimal surface to critical points of any energy. The index of a discrete surface can be used to classify a critical point as a minimum of a geometric energy. We also analyze the maximum principle of triangulated surfaces that are critical points of geometric energies. Besides that, we show that any additive locally supported geometric energy homogeneous of degree $2$ approximates the area of discrete surfaces. Chapter 4 contains the main results of the thesis.

Another example of additive geometric energy, but not locally supported, is the discrete Willmore energy, described in Chapter 5. The study presented here is based on a discrete version introduced in (1, 2), obtaining *discrete Willmore surfaces*. In this chapter, we also present an alternative discrete Willmore energy, that is another contribution of this thesis. This new energy does not satisfy the same properties satisfied by the discrete version cited previously, but its simple formulation and good results obtained by its implementation make this energy an interesting topic to future research.

This thesis is organized as follows. In Chapter 2, we review two important methods to find a minimum of a discrete function, namely the steepest descent method and a generalized Newton method. In Chapter 3, we start our study of geometric energies with an important and known example: the area functional. This chapter is completely based on previous works, specially (22). In Chapter 4 we introduce geometric energies. Some examples of additive locally supported geometric energies are provided and their properties are verified. Besides that, we prove the relation of geometric energies and discrete Laplacians. And finally in Chapter 5 we discuss the discrete Willmore energy.

# 2
# Preliminaries

There are many methods to optimize discrete functions. In this chapter we briefly discuss two methods: Steepest Descent and Newton, that will be used to minimize energies over triangulated surfaces in the following chapters. Besides that, we will establish a notation for the remainder of the thesis.

## 2.1
## Steepest Descent

This method is based on the time discretization and its basic idea is very simple, as its implementation. In a few words, let $f : \mathbb{R}^d \longrightarrow \mathbb{R}$ be a smooth function and $x_0 \in \mathbb{R}^d$ the initial approximation to a minimum of $f$. The sequence

$$x_{n+1} = x_n - dt\ \nabla_{x_n} f(x_n),$$

where $\nabla$ represents the gradient operator and $dt$ is a real number called *time step*, tend to converge to a minimum of $f$. Any term of this sequence is an approximation to a minimum of $f$ with some error.

This method is usually used on simple meshes, since if the triangulated surface were large, the time step restriction result in the need of hundreds of iterations to reach the minimum.

In next chapters we will consider energies defined on triangulated surfaces with $n$ vertices

$$E : \mathbb{R}^{3n} \longrightarrow \mathbb{R}.$$

The following steps will provide the minimum of $E$:

1. Choose an initial approximation to the minimum of $E$, denoted $M_0$, with $n$ vertices.

2. Given $M_i$ a triangulated surface with vertices $v_k^i$, $k = 1, \ldots, n$, the vertices $v_k^{i+1}$ of the surface $M_{i+1}$ are given by

$$v_k^{i+1} = v_k^i - dt\ \nabla_{v_k^i} E(M_i),$$

where $dt$ is the time step.

3. If $|E(M_i) - E(M_{i+1})| > \epsilon$ for a given $\epsilon$, return to step 2. Otherwise, $M_{i+1}$ is the approximation to a minimum of $E$.

The tolerance $\epsilon$ must be chosen in the beginning of the procedure as parameter for the method.

This method tends to converge to a minimal of $E$, since it just evolves with the initial surface in the direction of the function decreasing, i.e., against the gradient of the $E$. But the convergence in discrete case is not assured, since it can happen degenerate triangles during the minimization.

For further details about this method, we suggest (12).

## 2.2 Generalized Newton method

The generalized Newton method is an iterative method to find approximations to zeros of real or vector functions, given an initial approximation. This method is very efficient if the initial approximation is close to the zero, but the convergence, as in the steepest method, is not assured.

In short, given a function $f : \mathbb{R}^n \longrightarrow \mathbb{R}^n$ and $x_0 \in \mathbb{R}^n$, let

$$f(x) \approx f(x_0) + C(x - x_0)^t$$

be a linear approximation to $f(x)$, where $x \in \mathbb{R}^n$ and $C$ is a $n \times n$ matrix close to the Jacobian matrix at $x_0$. Then,

$$x \approx x_0 + C^{-1}\big(f(x) - f(x_0)\big)^t.$$

Considering that $x_0$ is an initial approximation to zero of $f$ and $x$ the zero of the linear approximation, we have

$$x \approx x_0 - C^{-1} f(x_0)^t.$$

In this sense, the sequence

$$x_{k+1} = x_k - C^{-1} f(x_k),$$

converges to a zero of $f$. So any $x_k$ is an approximation of the zero of $f$ with some error.

When $C$ is the Jacobian matrix of $f$ at $x_0$, we have the usual Newton method.

In our case, Newton method is used to find minimum of energies

$$E : \mathbb{R}^{3n} \longrightarrow \mathbb{R}.$$

So, we desire to get a zero of the following function

$$\begin{aligned} f: \ \mathbb{R}^{3n} &\longrightarrow \mathbb{R}^{3n} \\ M &\longmapsto (\nabla_{v_1} E, \ldots, \nabla_{v_n} E) \end{aligned}$$

using the generalized Newton method, where $n$ is the number of vertices of a triangulated surface $M$ and $v_i$ its vertices. The required matrix $C$ of the method will be explicitly determined in next chapters.

Now we present some steps used to implement this method.

1. Choose a initial approximation to zero of $f$, denoted $M_0$.

2. Given a triangulated surface $M_i$, the surface $M_{i+1}$ can be computed as

$$M_{i+1} = M_i - C^{-1}(\nabla_{v_1^i} E(M_i), \ldots, \nabla_{v_n^i} E(M_i))^t,$$

   where $v_1^i, \ldots, v_n^i$ are the vertices of $M_i$ and $n$ the number of vertices of $M_i$.

3. If $|E(M_i) - E(M_{i+1})| > \epsilon$ for a given $\epsilon$, return to 2. Otherwise, $M_{i+1}$ is the desired surface.

   To see details about this method, we suggest (12).

## 2.3 Notation

In the remainder of this thesis, we will use the following notation: $M$ is a triangulated surface with $n$ vertices, where $V = \{p \,|\, p = 1, \ldots, n\}$ is the set of vertex indices and $Edges(M)$ is the set of edges $e_{pq}$ of $M$ connecting $p$ and $q$ in $M$. The triangles in $M$ with vertices $p, q, r$ and edges $e_{pq}, e_{qr}, e_{rp}$ will be called $t_{pqr}$.

To simplify the notation, we use $p$ to represent the index of the vertex and to represent the location of vertex $p$ in space $\mathbb{R}^3$, i.e., $p = (p_x, p_y, p_z)$. Consequently, $\nabla_p F$ will denote the gradient of a functional $F$ with respect to the geometry of the vertex $p$.

Besides that, $N(p) = \{q \,|\, e_{pq} \in Edges(M)\}$ is the set of immediate neighbors of $p$ in the mesh and $d_p = |N(p)|$ is the number of them. $d_p$ is usually called degree or valence of $p$.

Finally, $T(p) = \{t_{pqr} \mid q, r \in N(p)\}$ is the set of triangles in $M$ formed by vertices $p$ and two neighbors of $p$.

# 3
# Area

*Plateau's problem* is the problem of finding a surface with minimal area among all surfaces that have the same prescribed boundary. This problem was named after the Belgium physicist J.A. Plateau who performed many experiments with soap films. The solution of this problem is called a *minimal surface*.

To find a solution of the Plateau's problem, it is necessary to minimize the area functional

$$\text{Area}(f) = \int_{\Omega} det(\text{Jacobian}(f)),$$

where $det$ is the determinant of the Jacobian matrix of $f$, in the class of parametric maps $f : \Omega \subset \mathbb{R}^2 \longrightarrow \mathbb{R}^3$ satisfying

$$f(\partial\Omega) = \Gamma,$$

for a given curve $\Gamma \subset \mathbb{R}^3$.

We are interested in finding solutions to a discrete version to Plateau's problem, i.e., we desire to get a triangulated surface with minimal area with a given boundary, in this case, a polygon. These surfaces will be called *discrete minimal surfaces*.

Numerically, there exist many methods to compute discrete minimal surfaces (4, 7, 10, 15, 31). We utilize here the method and algorithm proposed by Pinkall and Polthier in (21).

## 3.1
## Smooth Dirichlet energy and minimal surfaces

Before starting the discrete case, we recall some definitions and properties from the smooth case.

**Definition 1** *A surface is called minimal if it has the least area compared to nearby surfaces with the same boundary.*

The original interest by these surfaces comes from this variational property. Later on other interesting properties of this kind of surfaces had called attention of the researchers such as being critical point of Dirichlet energy and being characterized by a vanishing mean curvature.

Let $f : \Omega \subset \mathbb{R}^2 \longrightarrow \mathbb{R}^3$ be a parameterization of a surface $f(\Omega) \subset \mathbb{R}^3$. Thus, the area of $f(\Omega)$ is given by

$$\text{Area}(f) = \int_\Omega det(\text{Jacobian}(f))$$

and the Dirichlet energy of $f$ is defined as

$$E_D(f) = \frac{1}{2}\int_\Omega |\nabla f|^2,$$

where $\nabla$ represents the gradient operator and $|\cdot|$ the Euclidean norm. The Dirichlet energy differs from the area by one term that depends on the parameterization, called *conformal energy*. We have

$$\underbrace{\int_\Omega det(\text{ Jacobian }(f))}_{\text{surface area}} = \underbrace{\frac{1}{2}\int_\Omega |f_x|^2 + |f_y|^2}_{\text{Dirichlet energy}} + \underbrace{\frac{1}{2}\int_\Omega |Jf_x - f_y|^2}_{\text{conformal energy}},$$

where J denotes the rotation of $90^o$ in the tangent plane, and $f_x, f_y$ the partial derivatives of $f$. If $f$ is a conformal parameterization, we have

$$\text{Area}(f) = E_D(f).$$

More details on the topics of this section can be found in (9).

## 3.2 Discrete minimal surface

In this section, we will define the discrete minimal surface.

First of all, we recall that the area of a triangulated surface $M$ is the sum of the area of all triangles $T$ in $M$, i.e.,

$$\text{Area}(M) = \sum_{T \in M} \text{Area}(T).$$

It is very simple to see that

$$\text{Area}(T) = \frac{1}{4}\big(\cot\alpha|e_{qr}|^2 + \cot\beta|e_{rp}|^2 + \cot\gamma|e_{pq}|^2\big),$$

where $T$ is the triangle with edges $e_{qr}, e_{rp}, e_{pq}$ opposite to angles $\alpha, \beta$ e $\gamma$, respectively. Then the surface area of $M$ is given by

$$Area(M) = \frac{1}{4}\sum_{e_{pq} \in Edges(M)} (\cot\alpha_{pq} + \cot\beta_{pq})|p - q|^2, \qquad (3\text{-}1)$$

where $\alpha_{pq}, \beta_{pq}$ are angles opposite to edges $e_{pq}$, as in Figure 3.1.

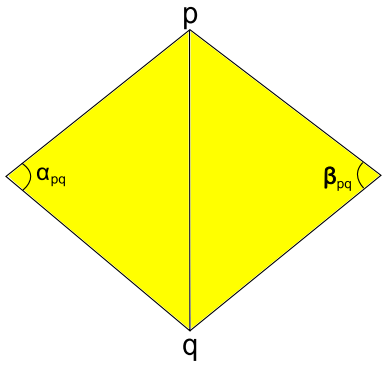


Figure 3.1: *Angles $\alpha_{pq}$ and $\beta_{pq}$ opposite to edge $e_{pq}$.*

With the given representation, we note that the area of $M$, is the weighted sum of all squared edges lengths from $M$, with weights depending only on the geometry of the adjacent triangles to the edge.

**Definition 2** *A triangulated surface $M$ is a discrete minimal surface if the area functional of $M$ is critical with respect to variations of any set of interior vertices of $M$.*

**Proposition 3** *A discrete minimal surface $M$ satisfies the following equation:*

$$\nabla_p Area = \frac{1}{2} \sum_{q \in N(p)} (\cot \alpha_{pq} + \cot \beta_{pq})(p - q) = 0, \tag{3-2}$$

*over all interior vertices $p$ of $M$, where $\alpha_{pq}, \beta_{pq}$ are opposite angles to edge $e_{pq}$ as in Figure 3.1.*

The proof of this proposition can be found in (22).

We remark that $\alpha_{pq}$ and $\beta_{pq}$ in Equation 3-1 changes with $p$. Therefore the gradient given by formula 3-2 is not so immediate to calculate as it seems at first.

The minimality condition above can be rewritten as

$$p = \frac{\sum_{q \in N(p)} (\cot \alpha_{pq} + \cot \beta_{pq}) q}{\sum_{q \in N(p)} \cot \alpha_{pq} + \cot \beta_{pq}}.$$

If this condition is true for all interior points $p$, then $M$ is a discrete minimal surface.

There are examples of discrete minimal surfaces described by its vertices. The discrete catenoid, for example, can be written in terms of hyperbolic cosine

function, as in the smooth case (see (24)) and discrete helicoid can be described in terms of hyperbolic sine (see (25)), also as in the continuous case.

The mean curvature vector on smooth surfaces provides a measure of how much the surface area changes compared to near surfaces, if a surface is moved at a constant speed along the surface normal. We would like to use a similar approach to obtain a discrete version, but there are many definitions of normal vector. In this case, we choose the area gradient among all possibilities to be faithful to the smooth case, as proposed in (22). In this sense, we have properties similar to the continuous case with respect to discrete mean curvature vector.

**Definition 4** *The discrete mean curvature vector of a vertex $p \in M$ is defined as*

$$\vec{H}\ (p) = \nabla_p Area(M).$$

*And the discrete mean curvature of $p \in M$ is the length of $\vec{H}\ (p)$, i.e.,*

$$H(p) = |\ \vec{H(p)}\ |.$$



To compute the total mean curvature of a surface, it is sufficient to add the discrete mean curvature of all vertices.

**Corollary 5** *A triangulated surface $M$ is a discrete minimal surface, if and only if, the discrete mean curvature vector vanishes at all vertices of $M$.*

## 3.3 Computing discrete minimal surfaces

In this section, we will show the method suggested by Pinkall and Polthier in (21), that aim at approximating a discrete minimal surface $M$ by a sequence of triangulated surfaces that converges to the minimum of the area. This is a generalized Newton method as defined in section 2.2.

Pinkall and Polthier defined a discrete version to Plateau's problem in the following way: given a fixed polygonal boundary $\Gamma$, determine a triangulated surface $M$ such that $\partial M = \Gamma$ satisfying

$$\nabla_p \text{Area}(M) = \frac{1}{2} \sum_{q \in N(p)} (\cot \alpha_{pq} + \cot \beta_{pq})(p - q) = 0$$

to all interior vertices $p$ in $M$, that is the minimality condition 3-2 for surface $M$. We shall use the generalized Newton method with the linear approximation to gradient given by Equation 3-2 with parameters $\alpha_{pq}, \beta_{pq}$ fixed.

Let us show how to determine the geometry of the interior vertices of $M$ explicitly. We denote the geometry of the vertex $i$ by $v_i$.

Let $M_0$ be an initial approximation to $M$ with vertices

$$M_0 = \{\underbrace{v_1, \ldots, v_i}_{interior(M_0)}, \underbrace{v_{i+1}, \ldots, v_{i+b}}_{boundary(M_0)=\Gamma}\}$$

and

$$M = \{\underbrace{x_1, \ldots, x_i}_{interior(M)}, \underbrace{v_{i+1}, \ldots, v_{i+b}}_{boundary(M)=\Gamma}\}$$

the vertices of $M$.

$M$ must satisfy the condition 3-2, then interior vertices $x_k$ of $M$, $1 \leq k \leq i$, can be obtained solving the linear system

$$\sum_{j=1}^{i} s_{kj} x_j + \sum_{j=i+1}^{i+b} s_{kj} v_j = 0, \text{ for } 1 \leq k \leq i$$

where

$$s_{kj} = \begin{cases} \text{if } k \neq j \text{ , then } \begin{cases} 0 \text{ , if } k \text{ is not adjacent to } j \\ -\frac{1}{2}(\cot \alpha_{kj} + \cot \beta_{kj}) \text{ , if } k \text{ is adjacent to } j \end{cases} \\ \text{if } k = j \text{ , then } s_{kk} = \sum_{j \in N(p_k)} (-s_{kj}) \end{cases} \tag{3-3}$$

recalling that $\alpha_{kj}$, $\beta_{kj}$ are the opposite angles to edges connecting vertices $k$ and $j$, where $1 \leq k, j \leq b + i$. The above linear system can be written in matricial form by

$$Ax = b \tag{3-4}$$

where $A$ denotes the $i \times i$ matrix with entries $a_{kj}$ given by

$$a_{kj} = s_{kj}$$

with $k, j = 1, \ldots, i$ and $b$ a column vector defined by

$$b_k = -\sum_{j=1+i}^{i+b} s_{kj} v_j.$$

Note that the matrix $S$ defined by entries $s_{kj}$, is positive definite. In fact, if $0 \geq M_0^t S M_0 \Leftrightarrow 0 \geq \text{Area}(M_0) \Leftrightarrow M_0 = 0$. Therefore the matrix $A$, obtained

taking off the same rows and columns from $S$ will be also positive definite. In this way, the linear system $Ax = b$ has a unique solution. And, actually, the Plateau's problem is solved minimizing the area functional, that is a quadratic problem and has an unique solution.

The algorithm applies recursively the previous step, and a sequence of discrete surface satisfying equation 3-2 is used to approximate the discrete minimal surface.

Let us enumerate the computational steps used to implement the method.

1. Choose an initial approximation to the discrete minimal surface, denoted $M_0$. This triangulated surface must have the prescribed boundary $\Gamma$.

2. Let $M_i$ be a triangulated surface satisfying $\partial M_i = \Gamma$. Compute the surface $M_{i+1}$ satisfying $\partial M_{i+1} = \Gamma$ such that

$$\nabla_p \text{Area}(M_{i+1}) = \frac{1}{2} \sum_{q \in N(p)} (\cot \alpha_{pq} + \cot \beta_{pq})(p - q) = 0,$$

   over all interior vertices $p$ in $M_{i+1}$, where $\alpha_{pq}, \beta_{pq}$ are opposite angles to edge $e_{pq}$ in $M_i$, as in Figure 3.1.

3. If $|\text{Area } (M_i) - \text{Area } (M_{i+1})| > \epsilon$ for a given $\epsilon$, then return to Step 2. Otherwise, $M_{i+1}$ is an approximate for a desired discrete minimal surface.

Note that, to execute step 2 it is necessary to solve a linear system as 3-4 and we get a new surface. If the new surface satisfies the desired tolerance in relation to the previous surface, it will be a new approximation of the desired discrete minimal surface. Against, step 2 must be repeated. The tolerance $\epsilon$ must be chosen in the beginning of the procedure.

**Proposition 6** *The algorithm converges to a solution of the problem, if the sequence of the surfaces $M_i$ does not have degenerate triangles.*

This proof can be found in (22).

The Plateau's problem can also be solved with the steepest descent method shown in Section 2.1, since we have an explicit description of the gradient of the area functional, given by equation 3-2. In this case, the implementation is very easy and it is not necessary to solve any system in each iteration. On the other side, the convergence is not so fast and the choice of $dt$ required by the method can be a problem.

## 3.4 Results

In this section, we will show results of computed discrete minimal surfaces from Plateau's problem. We utilize here the steepest descent method and generalized Newton method as described in previous section.

In the next figures we can see the energy value of the triangles star of each vertex, represented by color maps, where blue represents the region with lower energy and red region with higher energy.

*Result 1:*

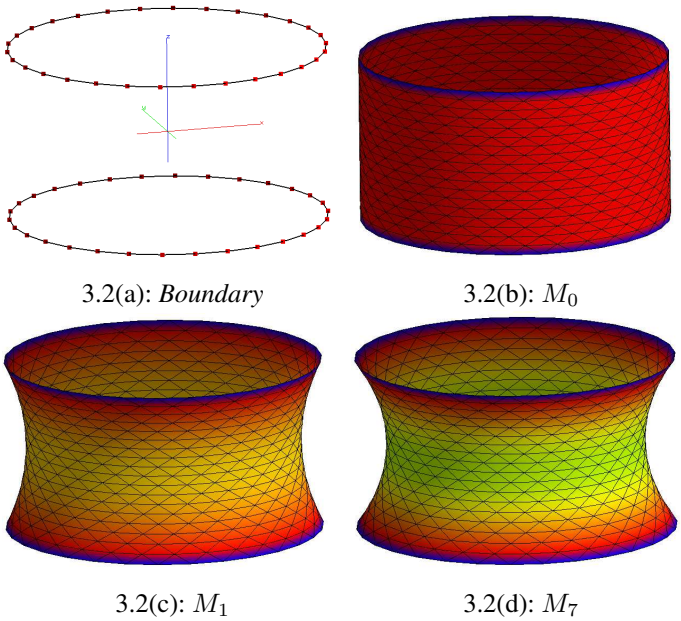

3.2(a): *Boundary* 3.2(b): $M_0$

3.2(c): $M_1$ 3.2(d): $M_7$

Figure 3.2: *Minimization of area over a cylinder.*

To get a discrete catenoid, the discrete cylinder (Figure 3.2(b)) with $570$ vertices bounded by two near, identical and aligned circles with $60$ vertices (Figure 3.2(a)) was chosen to initial approximation. The ratio between radius and height of the cylinder is $0,925$. Note that, the circles are sufficiently close to avoid degeneracies of the triangles, as in the smooth case; and because of that, the catenoid obtained can be called stable. Figure 3.2(c) is a solution of the first iteration of the minimization of the area functional with the generalized Newton method over a discrete cylinder, i.e., only one sparse linear system was solved to a initial surface. As we said before, the Newton method converges quickly, and because of that, in that Figure 3.2(c) it is possible to see a surface similar to a catenoid. In this case, the convergence happens with $7$ iterations, i.e., only $7$ linear systems as 3-4 were solved. Figure 3.2(d) is the solution of the discrete Plateau's problem, given two identical and aligned circles as boundary.

The distance between the circles of the boundary is very important, and the stability of the final catenoid it depends on that. In the next example, we show one case with not so close circles.

*Result 2:*

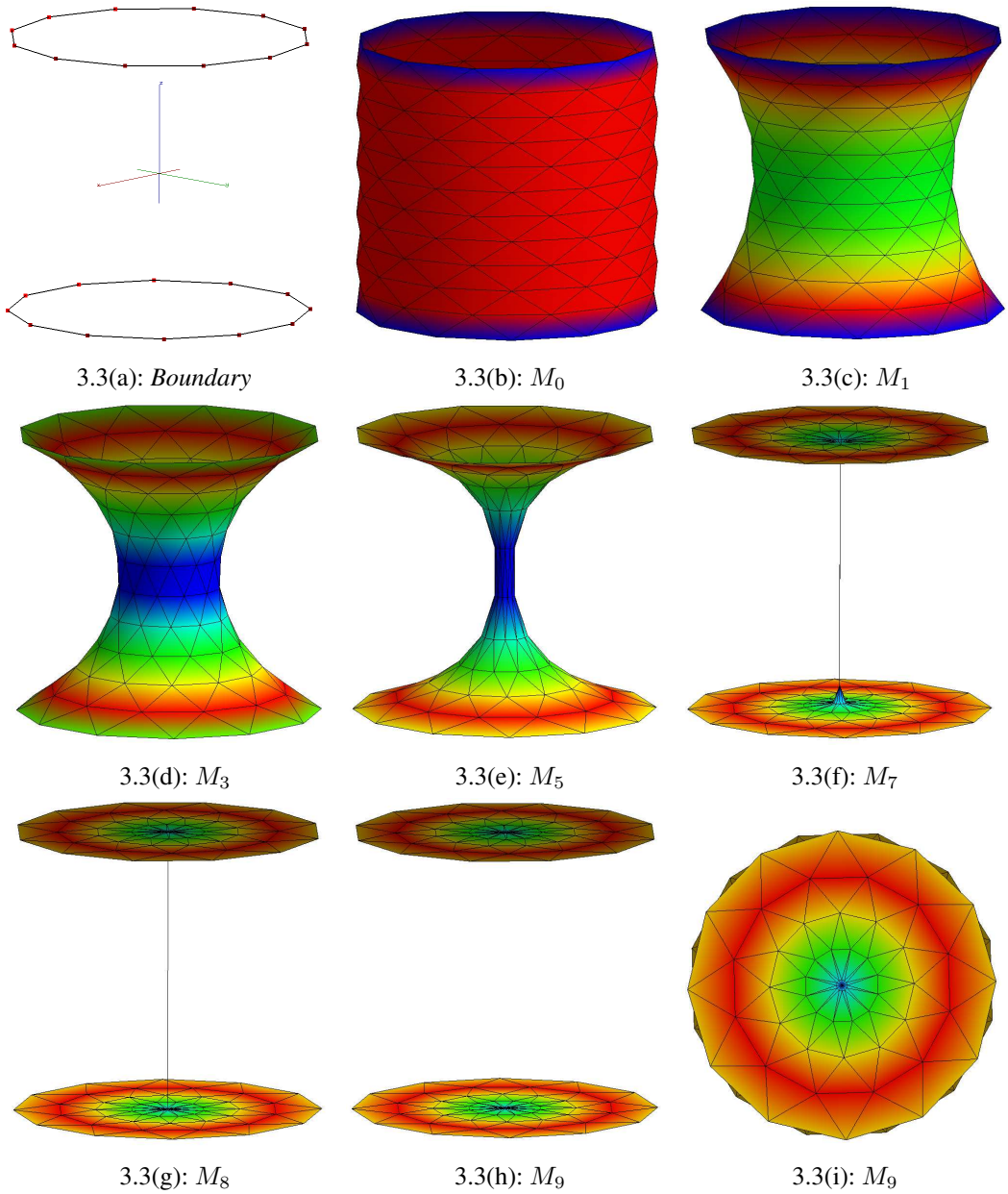

3.3(a): *Boundary* 3.3(b): $M_0$ 3.3(c): $M_1$

3.3(d): $M_3$ 3.3(e): $M_5$ 3.3(f): $M_7$

3.3(g): $M_8$ 3.3(h): $M_9$ 3.3(i): $M_9$

Figure 3.3: *Minimization of area over another cylinder.*

As we said, we take once again two identical and aligned circles with 24 vertices to boundary of a discrete minimal surface, given in Figure 3.3(a). In this case the distance between the circles is bigger than the previous case, therefore the ratio between radius and height of the cylinder is $0,0,543$. The initial approximation is another discrete cylinder with $144$ vertices, shown in Figure 3.3(b). Figure 3.3

shows some steps of the minimization of area functional over that cylinder. Our goal is to get a unstable catenoid, i.e., a catenoid without degenerate triangles.

In (21), the degeneracy of the triangles is discussed. The suggestion to solve this problem is to take off the degenerated triangles and to proceed normally with the minimization until we get the given tolerance. In this example, we follow this suggestion.

*Remark:* Degenerate triangle means that triangle angles become $0$ or $\pi$. This happens when the triangle shrinks to a line, i.e., all three point becoming collinear, or two or three vertices merge to a single point.

Note that, the height of the interior triangles of the cylinder increases quickly, providing degenerate triangles. In Figure 3.3(g), we can see clearly a degenerated triangle that connects two different parts of the surface. In this step this triangle is eliminated and the procedure follows. The result of the next iteration is our desired surface: unstable catenoid, Figure 3.3(h). This result was obtained in the end of $9$ iterations of the Newton method. In Figure 3.3(i) we have the final surface shown from the top.

*Result 3:*

In this result, the boundary chosen for the Plateau's problem is only one disk with 16 vertices, as we can see in Figure 3.4(a) and the initial approximation to the desired discrete minimal surface is a half-sphere with $129$ vertices, shown in Figure 3.4(b). In this case, only one minimization step leads directly to a planar surface of Figure 3.4(c).

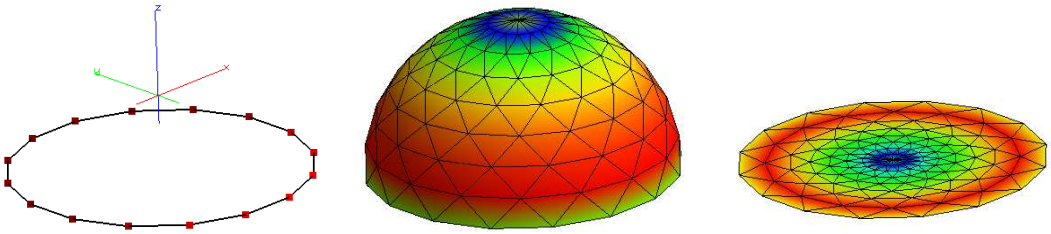

3.4(a): *Boundary* 3.4(b): $M_0$ 3.4(c): $M_1$

Figure 3.4: *Minimization of area over a half-sphere.*

*Result 4:*

In Figure 3.5 we present the results obtained by the minimization procedure of the area functional over a surface whose boundary is formed by $3$ circles with 96 vertices, as in Figure 3.5(a). This example is similar to the second example shown previously, where some triangles degenerate. In Figure 3.5(b) we can see an initial approximation with $451$ vertices to the desired minimal surface, in this case a discrete trinoid. The triangulation of the initial surface has triangles with different areas, as illustrated by the colors of the surface. In this example, we see once again the instability of the area functional, since some triangles degenerate. The figure obtained without eliminating the degenerate triangles is shown in Figure 3.5(e), and from another point of view, Figure 3.5(f).

In this example, we use the steepest descent method described in Section 2.1, where the parameters are: tolerance $\epsilon = 10^{-2}$ and the time step $dt = 10^{-5}$.

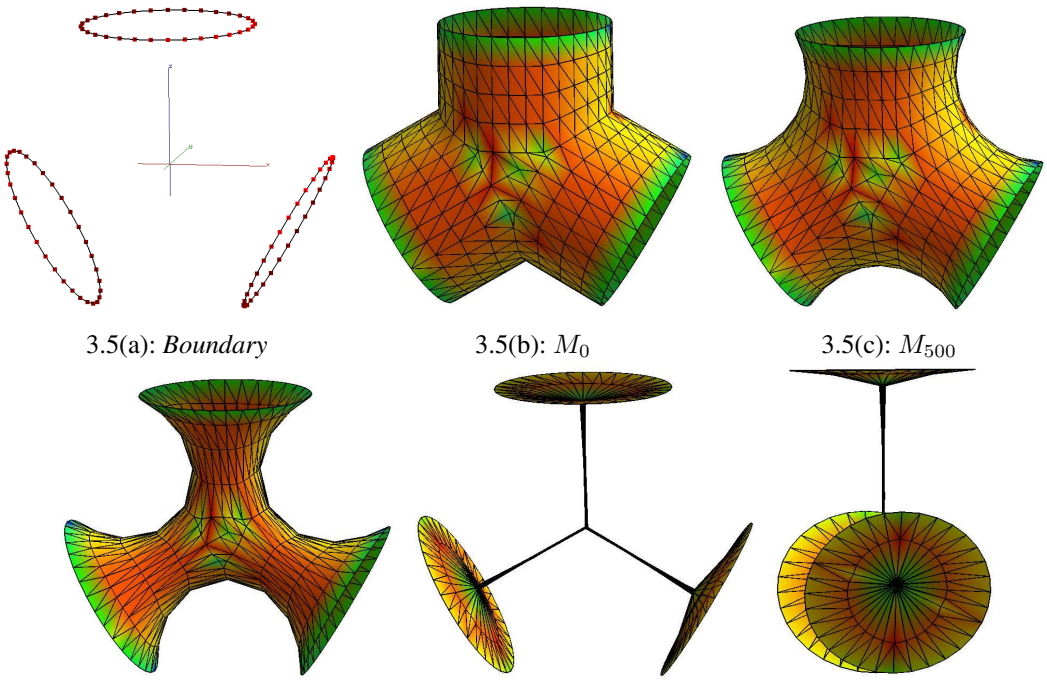

3.5(a): *Boundary* 3.5(b): $M_0$ 3.5(c): $M_{500}$

3.5(d): $M_{2000}$ 3.5(e): $M_{5000}$ 3.5(f): $M_{5000}$

Figure 3.5: *Minimization of area over a triangulated surface 3.5(b).*

# 4
# Geometric energies based on triangles

In Numerics and Computers Graphics, there exist many methods based on energy minimization. The choice of a suitable energy depends on the desired application. In the previous chapter, for example, area functional was used to compute discrete minimal surfaces.

We consider here energies defined on discrete triangulated surfaces satisfying some suitable properties. The main property is invariance under rigid motions. We shall call any energy with this property a *geometric energy*. Another important property is a *local support*. This means that the energy of a single triangle depends only on its geometry and not on the triangles of its neighborhood. Finally, we shall call the energy *additive* if the energy of the surface is the sum of the energy of each triangle.

In this chapter, we present definition, properties and examples of additive locally supported geometric energies, as well as its applications. Any such energy

$$\begin{aligned} E: \ \mathbb{R}^{3n} &\longrightarrow \mathbb{R} \\ M &\longmapsto E(M) \end{aligned}$$

where $n$ is the number of vertices of the triangulated surface $M$, can be written as

$$E(M) \ = \ \sum_{t_{ijk} \in M} f(t_{ijk}),$$

where $t_{ijk} \in M$ are triangles of $M$.

The invariance under rigid motions implies that

$$f(t_{ijk}) = f(l_{ij}, l_{jk}, l_{ki}),$$

such that $l_{ij}, l_{jk}, l_{ki}$ are the sides of the triangle $t_{ijk} \in M$ (see (5)). Besides that, $f$ is invariant under permutation of its arguments, i.e.,

$$f(l_{ij}, l_{jk}, l_{ki}) = f(l_{ki}, l_{ij}, l_{jk}).$$

This formulation allows us to establish a simple and efficient framework which

computes the gradient, Hessian, indices of surfaces and proves general properties of geometric energies. We also relate geometric energies and discrete Laplacians defined in (34) by

$$L(p) = \sum_{q \in N(p)} \omega_{pq}(p - q),$$

where $p$ is a vertex of the discrete surface $M$ and $\omega_{pq}$ is a weight given to the edge connecting vertices $p$ and $q$. This relation will be presented in this chapter.

In the remainder of this thesis, we will refer to a triangle $T = (p, q, r)$ in $M$ with angles $\alpha, \beta, \gamma$ as in the Figure 4.1.

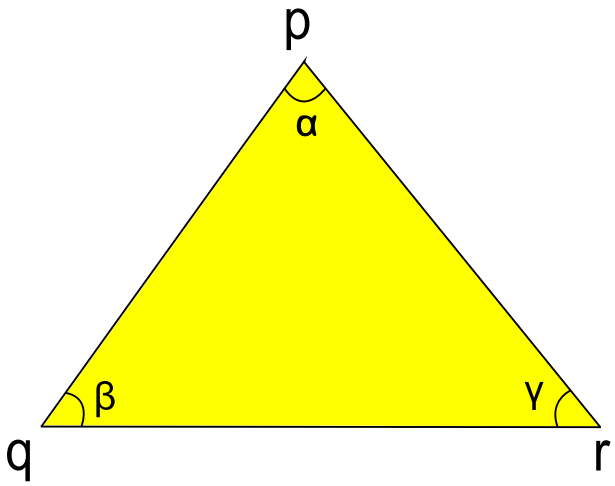


Figure 4.1: *Triangle $T$ in a triangulated surface $M$.*



## 4.1 Some examples of additive locally supported geometric energies

In this section we will present some examples of additive locally supported geometric energies and results obtained by their minimization.

### 4.1.1 Area

The area of $M$, defined in Chapter 3 by Equation 3-1 is a locally supported geometric energy. In this chapter, this energy will be denoted $E_1$.

$E_1$ can be calculated in different ways, among them:

$$E_1(M) = \sum_{T \in M} \cot\alpha |r - q|^2 + \cot\beta |p - r|^2 + \cot\gamma |q - p|^2,$$

where $T$ is a triangle with angles $\alpha, \beta, \gamma$ and vertices $p$, $q$ and $r$ (see Figure 4.1).

Equivalently we can write

$$E_1(M) = \sum_{T \in M} \left( \frac{\sin\beta \sin\gamma}{\sin\alpha} \right) |q - r|^2.$$

$E_1$ is a very important tool for the construction of discrete minimal surfaces, as we presented in the previous chapter. Furthermore, this energy appears in many papers being used to obtain the Laplacian of the cotangents of the mesh. For applications we suggest (18, 19, 26).

Results provided by the minimization procedure of $E_1$ are also in Chapter 3.

### 4.1.2 Squared edges energy

The squared edges energy of a triangulated surface $M$, denoted $E_2$, is given by

$$E_2(M) = \sum_{e_{pq} \in Edges(M)} |e_{pq}|^2.$$

We can also write this energy as

$$E_2(M) = \frac{1}{2} \sum_{T \in M} |p - q|^2 + |q - r|^2 + |r - p|^2,$$

where $T$ is a triangle with vertices $p, q, r$ in $M$.

The gradient of $E_2$ can be easily computed as

$$\nabla_p E_2(M) = \sum_{q \in N(p)} (p - q).$$

So, the discrete surface $M$ is a minimum of $E_2$ if it satisfies

$$\nabla_p E_2(M) = 0$$

over all vertices $p$ in $M$, or equivalently,

$$p = \frac{1}{d_p} \sum_{q \in N(p)} q. \tag{4-1}$$

If the above condition is satisfied, vertex $p$ lies at the center of gravity of its immediate neighbors, distributing the vertices over the space in a good way.

Considering the minimally condition for all vertices in $M$, the condition 4-1 becomes in the following matricial form:

$$Lv_x = 0, Lv_y = 0, Lv_z = 0$$

where $v_x, v_y, v_z$ represent the vectors composed by coordinates $x, y, z$, respectively, of the entire mesh and $L$ is a $n \times n$ matrix with entries:

$$l_{pq} = \begin{cases} d_p & , \text{ if } p = q \\ -1 & , \text{ if } e_{pq} \in Edges(M) \\ 0 & , \text{ otherwise.} \end{cases}$$

The matrix $L$ is known as the *Combinatorial Laplacian* of the mesh, as we can find in (17, 20, 27, 30, 34, 37). This Laplacian is very useful due to its simple definition using only the connectivity of the mesh. Besides that, matrix $L$ is symmetric, and so it has real eigenvalues and orthogonal eigenvectors.

There is a different Laplacian using only the connectivity of the mesh, called the *Tutte Laplacian*. In this case the Laplacian matrix $\bar{L}$ is given by

$$\bar{l}_{pq} = \begin{cases} 1 & , \text{ if } p = q \\ -1/d_p & , \text{ if } e_{pq} \in Edges(M) \\ 0 & , \text{ otherwise.} \end{cases}$$

In (14, 16, 19, 28, 29, 32, 34, 37) we can find details about the Tutte Laplacian and its applications.

An example of the mesh smoothing using $E_2$ is shown in Figure 4.2. Figure 4.2(a) shows the original bi-torus with 2174 vertices with sharp edges, that will be removed during the minimization of $E_2$. Each vertex is colored according to energy value of its star, where color blue represents the region with lower energy value and color red with higher value. The triangulation allows to see the variation of the energy in adjacent regions with different triangulations. Figures 4.2(b), 4.2(c), 4.2(d) show some steps of the minimization of $E_2$, using steepest descent method defined in Section 2.1. The time step used in the method is $0,01$. Note that, Figure 4.2(d) has more homogeneous distribution of energy. However, there is a region with high energy value around some vertices (red region), since the adjacent edges to this vertex are bigger than the others. The mesh shown in Figure 4.2(d) was obtained after 240 iterations of steepest descent method.

Note that our goal with this minimization is to smooth the original mesh given in Figure 4.2(a). In this case, the number of iterations of this procedure is chosen according to desired smoothness. But, it is clear that too many iterations can make the original mesh disappeared. To control this problem, it is sufficient to keep some vertices fixed. By keeping some vertices fixed it is also possible to use Newton method, by solving an analog system to 3-4, replacing the matrix $S$ to

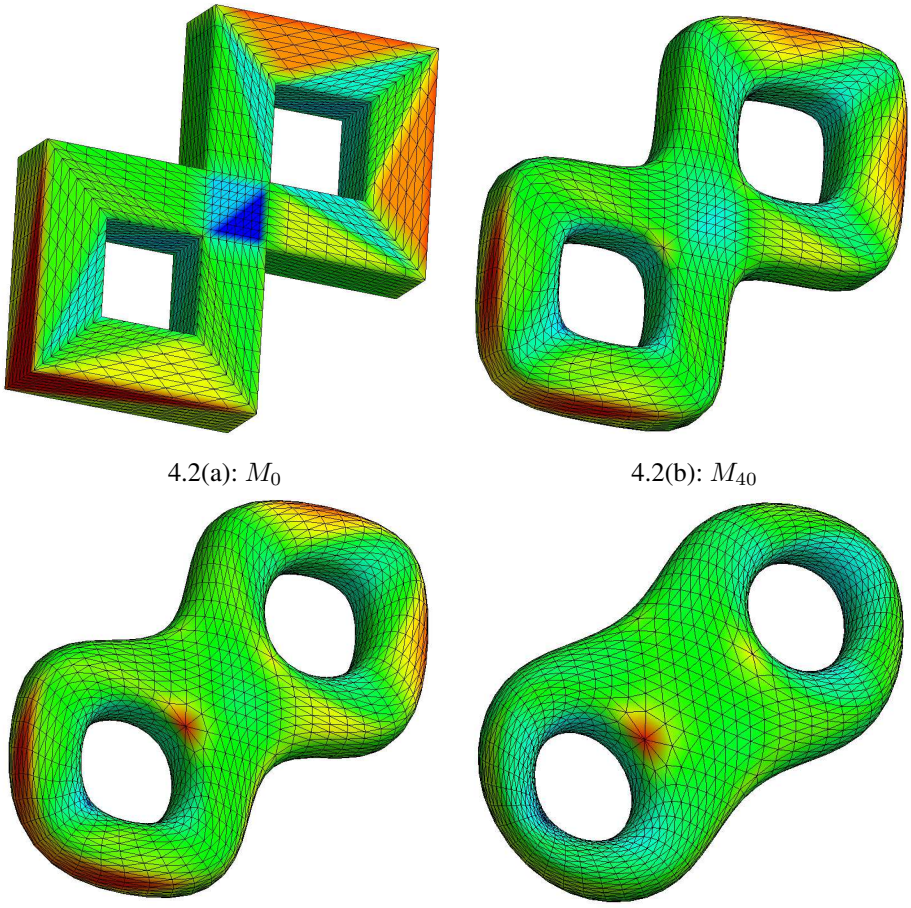

4.2(a): $M_0$ 4.2(b): $M_{40}$

4.2(c): $M_{100}$ 4.2(d): $M_{240}$

Figure 4.2: *Minimization of $E_2$ over a bi-torus.*

Laplacian matrix $L$ or $\bar{L}$.

Isenburg et al. (14) shows how to compute the geometry of the entire mesh from $E_2$ with a prescribed connectivity, assuming uniform edge length and smoothing. In this case, a unit sphere, with the same number of vertices and the same connectivity as the final mesh, is the initial approximation. They minimize the sum of two energies, and one of them is $E_2$. This shows the amount of geometric information implicit in the connectivity.

### 4.1.3 Circumscribed radius energy

In this section we introduce a new energy constructed with the radius of the circumscribed circles of the triangles of the discrete surface, and we denote it by $E_3$. Its goal is to provide surfaces containing triangles close to equilateral, improving the quality of the mesh and the visualization of the details.

The quality of the mesh will be measured with the value of the *aspect ratio* of

the triangles $T$, as the Figure 4.1, given by

$$AR(T) = \frac{4\sqrt{3}\,\text{Area}(T)}{|e_{pq}|^2 + |e_{qr}|^2 + |e_{pr}|^2}.$$

Note that $0 < AR(T) \leq 1$, and if the triangle is equilateral, the aspect ratio is 1.

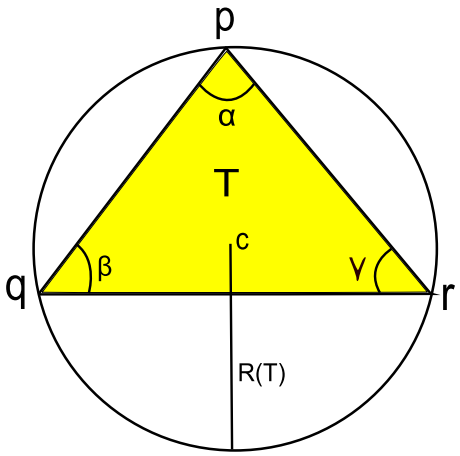


Figure 4.3: *Circle with radius $R(T)$ circumscribed to a triangle $T$.*

Let $R(T)$ be the radius of the circumscribed circle of the triangle $T$, as in Figure 4.3. The circumscribed radius energy of the triangulated surface $M$ is given by

$$E_3(M) = \sum_{T \in M} R^2(T).$$

Following the law of sines

$$\frac{|p-q|}{\sin\gamma} = \frac{|p-r|}{\sin\beta} = \frac{|q-r|}{\sin\alpha} = 2R(T),$$

so there are different ways to compute $E_3$. For example, we can write

$$E_3(M) = \sum_{T \in M} \frac{|q-r|^2}{4\sin^2\alpha}.$$

In the next section, we shall prove that its gradient takes the form

$$\nabla_p E_3(M) = \sum_{t_{pqr} \in T(p)} \left(\frac{\cot\alpha\cot\beta}{2\sin^2\gamma}\right)(p-q) + \left(\frac{\cot\alpha\cot\gamma}{2\sin^2\beta}\right)(p-r).$$

This equation represents the gradient of $E_3$ with respect to a vertex $p$, given by the sum over the adjacent edges to $p$ with a weight. In this case, we note that the weights are functions of the angles of the adjacent triangles of $p$.

From the numerical point of view, since we have already computed the gradient of $E_3$, it is very easy to minimize $E_3$. In the following, we present some

results provided minimizing the energy $E_3$ over discrete surfaces satisfying the Dirichlet condition (keeping fixed boundary). We choose the boundary curves and the initial approximation for the surfaces that we have already used in Chapter 3, shown in Figures 3.2, 3.3, 3.4, 3.5.

The colors of the next figures represent the energy $E_3$ value, computed in the triangles star of each vertex, where blue is the lower energy $E_3$ value and red the higher $E_3$ value energy.

The next results were obtained with the steepest descent method, with the following parameters: tolerance $\epsilon = 10^{-5}$ and time step $dt = 0,01$.

*Result 1:*

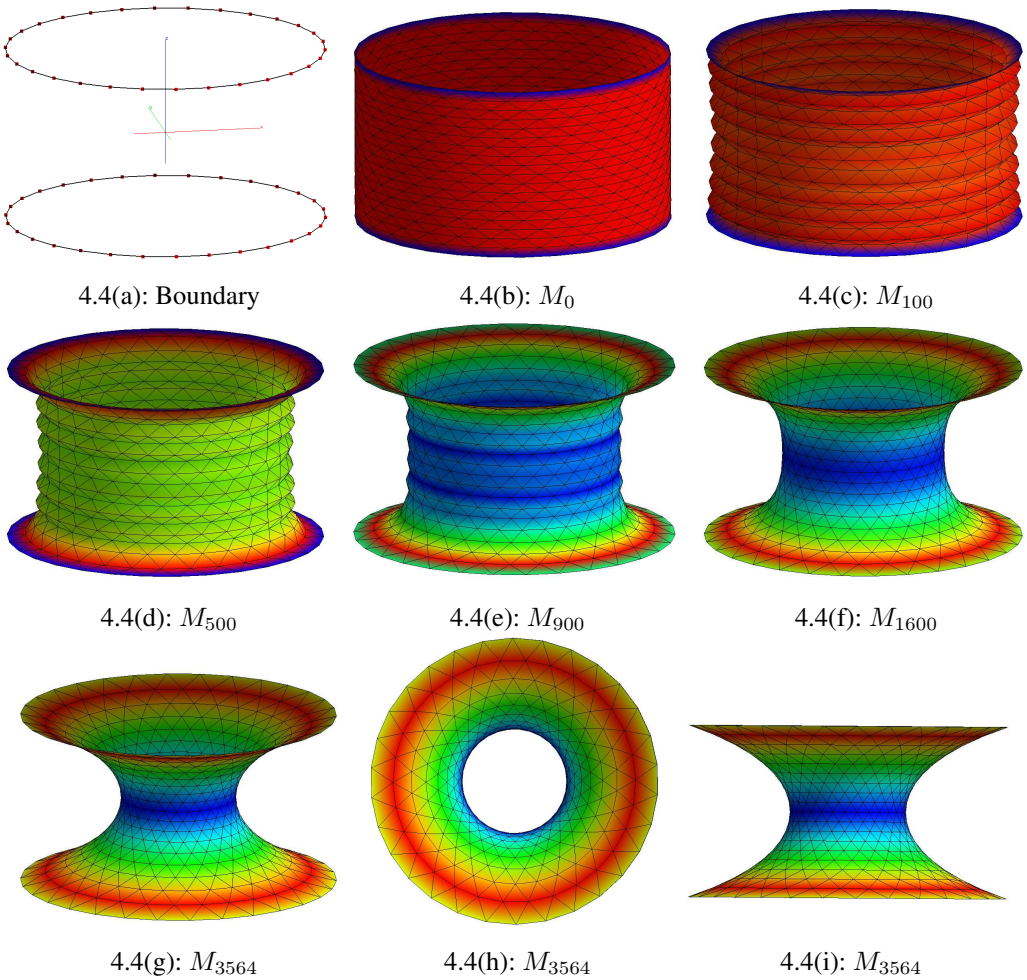

4.4(a): Boundary 4.4(b): $M_0$ 4.4(c): $M_{100}$

4.4(d): $M_{500}$ 4.4(e): $M_{900}$ 4.4(f): $M_{1600}$

4.4(g): $M_{3564}$ 4.4(h): $M_{3564}$ 4.4(i): $M_{3564}$

Figure 4.4: *Minimization of $E_3$ over a cylinder.*

In Figure 3.2 we got a discrete catenoid minimizing $E_1$ or area functional over a cylinder with $570$ vertices, being $70$ on the boundary. The next result was obtained minimizing the energy $E_3$ over the same cylinder, that it can be seen in Figure 4.4(b) and its boundary in Figure 4.4(a). Figures 4.4(c), 4.4(d), 4.4(e), 4.4(f)

show some iterations of the procedure. Surfaces obtained before the convergence can have sharp regions, as in Figures 4.4(c), 4.4(d), but these regions are quickly removed, converging to a smooth discrete surface, Figure 4.4(g). Figures 4.4(i) and 4.4(h) show the final surface from others points of view.

The surfaces shown in Figures 3.2(d) and 4.4(g) are similar, however the first one is a discrete catenoid, obtained by area minimization, and the last one is a surface provided by minimization of $E_3$.

The goal of energy $E_3$ is improve the aspect ratio of the triangulated surfaces. To show this improvement, we present a histogram with the triangles aspect ratio in some iterations of the minimization procedure described previously. The horizontal axis of the histogram is used to the value of the triangles aspect ratio and the vertical axis, to the number of the triangles. The blue rectangle represents the initial cylinder (Figure 4.4(b)), the red rectangles represent the surface obtained after $100$ iterations of the steepest descent and finally, the green rectangle represents the final surface (Figure 4.4(g)) obtained after $3564$ iterations. In this histogram we see clearly the improvement of the triangles aspect ratio during the minimization of the energy $E_3$, and the final surface (Figure 4.4(g)) has all triangles with aspect ratio close to $1$, i.e., all triangles are close to equilateral.

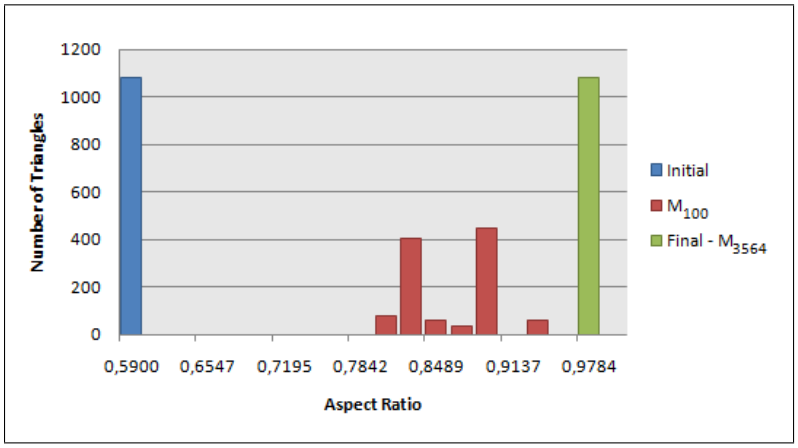


Figure 4.5: *Histogram of the triangles aspect ratio of the surfaces obtained by minimization of $E_3$ over a cylinder, shown in Figure 4.4.*

In Figure 4.6, we see a graphic with mean, maximum and minimum of the triangles aspect ratio of the surfaces, obtained in each iteration of the steepest descent method (shown in Figure 4.4). The horizontal axis shows the number of the iterations and the vertical axis shows the value of the aspect ratio. Note that mean, maximum and minimum of the triangles aspect ratio of the surfaces tend to 1.

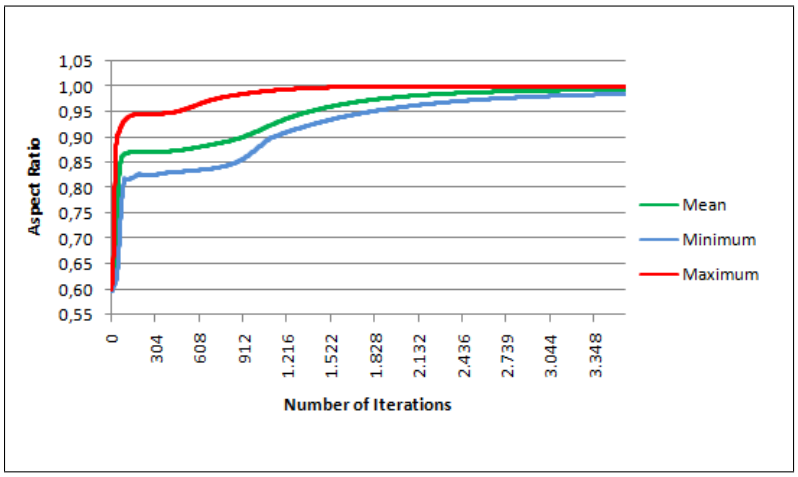


Figure 4.6: *Graphic of the mean, minimum and maximum triangles aspect ratio of each iteration in minimization of $E_3$ over a cylinder, shown in Figure 4.4.*

*Result 2:*

The minimization of the area over a different cylinder is shown in Figure 3.3. In that case, the cylinder had $144$ vertices, where boundary is given by two circles also aligned with $24$ vertices, but not so close as in the previous result. Degenerate triangles were excluded during the minimization and the procedure followed, converging to a unstable discrete catenoid. In Figure 4.4, we will show the minimization result of $E_3$ over the same cylinder. Figures 4.4(a) and Figure 4.4(b) shows the boundary and the initial approximation, respectively, used before. Surfaces provided from iterations of the steepest method are shown in Figures 4.7(c), 4.7(d) and the final surface is shown in Figure 4.7(e) or 4.7(f) (from the top).

In this case, we have fixed the number of vertices of the initial approximation, and degenerate triangles did not appear. This result is completely different from the result provided by the minimization of $E_1$ over the same discrete surface, which shows the interest of energy $E_3$.

In the histogram of the Figure 4.8, which shows triangles aspect ratio in some iterations of this minimization, we can see the quality of the triangles obtained in the end of the procedure. The horizontal axis is used to the value of the aspect ratio and the vertical axis, to the number of the triangles. The blue rectangle represents the initial cylinder (Figure 4.7(b)), red rectangles represent the surface obtained after $22$ iterations of the steepest descent and green rectangles represent the final surface obtained after $1226$ iterations (Figure 4.4(g)). The final surface has triangles aspect ratio completely different from the initial surface, being closer to 1 than the triangles aspect ratio of initial cylinder.

Let us show a analogous graphic of the Figure 4.6 to this minimization. In

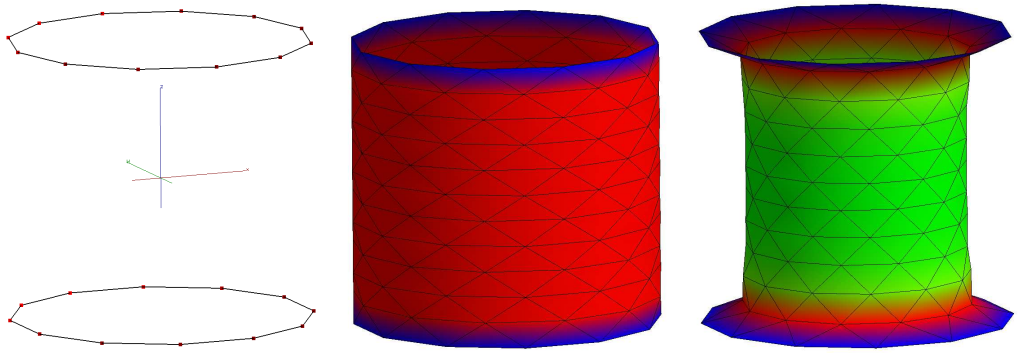

4.7(a): Boundary 4.7(b): $M_0$ 4.7(c): $M_{100}$

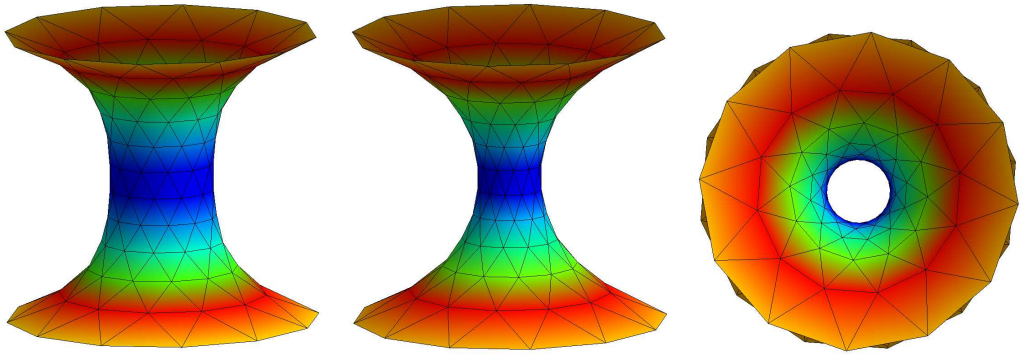

4.7(d): $M_{500}$ 4.7(e): $M_{1226}$ 4.7(f): $M_{1226}$

Figure 4.7: *Minimization of $E_3$ over another cylinder.*

Figure 4.8, we have mean, maximum and minimum of the aspect ratio triangles of each iteration of the steepest descent method, shown in Figure 4.7. In this case, the result is not so good as previous result, but it is clear the improvement of the triangles aspect ratio of the surfaces.

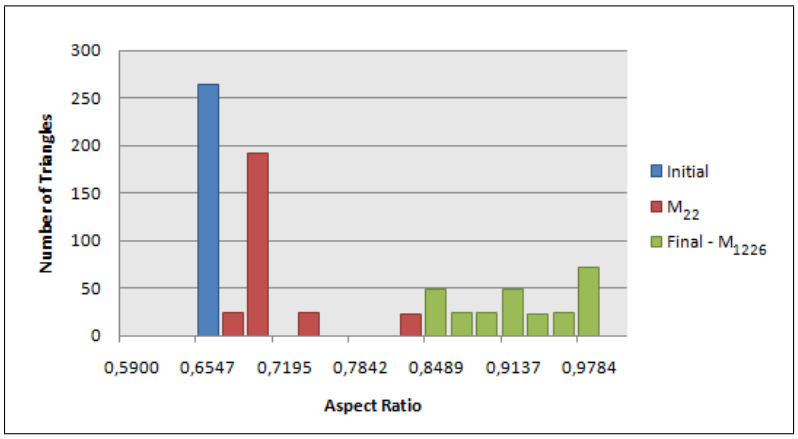


Figure 4.8: *Histogram of the triangles aspect ratio of the surfaces obtained by minimization of $E_3$ over another cylinder, shown in Figure 4.7.*

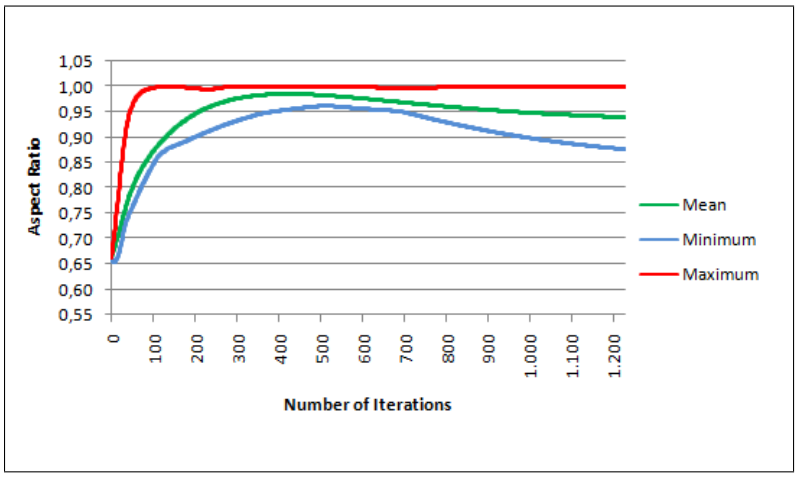


Figure 4.9: *Graphic of the mean, minimum and maximum triangles aspect ratio of the each iteration of the minimization of $E_3$ over another cylinder, shown in Figure 4.7.*

*Result 3:*

In this example, the mesh has 129 vertices, being 16 on the boundary, and it is equal to the half-sphere shown in Figure 3.4. In contrast to the previous chapter, we have minimized energy $E_3$ over this mesh with steepest descent method. Figures 4.10(c) and 4.10(d) show the intermediate steps of the procedure and finally Figure 4.10(e) shows a minimum of $E_3$, over all surfaces with the same circle as boundary. In Figure 4.10(f) it is clear the regularity of the triangles, and near the boundary the triangles have higher circumscribed radius, so this region has the higher energy $E_3$ value, as shown in red color. Note that, Figures 3.4(c) and 4.10(e) are similar.

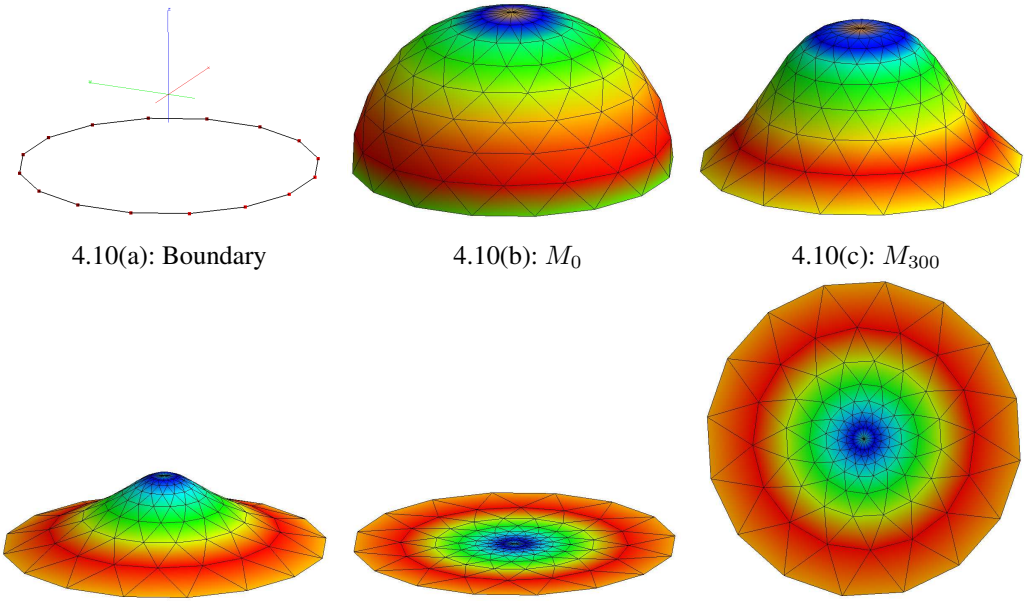

4.10(a): Boundary 4.10(b): $M_0$ 4.10(c): $M_{300}$

4.10(d): $M_{2000}$ 4.10(e): $M_{5863}$ 4.10(f): $M_{5863}$

Figure 4.10: *Minimization of $E_3$ over a half-sphere.*

The triangles aspect ratio of some surfaces obtained in minimization shown in the Figure 4.10 can be seen in histogram of the Figure 4.11. The horizontal axis is used to the value of the aspect ratio and the vertical axis, to the number of the triangles. The blue rectangle represents the initial cylinder (Figure 4.10(b)), the red rectangles represent the surface obtained after $50$ iterations of the steepest descent and the green rectangle represents the final surface obtained after $5863$ iterations and shown in Figure 4.10(e). In this case, closer to $1$ there is a higher concentration of the triangles of the final surface, represented by green rectangle, which shows the improvement of the triangles aspect ratio with the minimization of $E_3$.

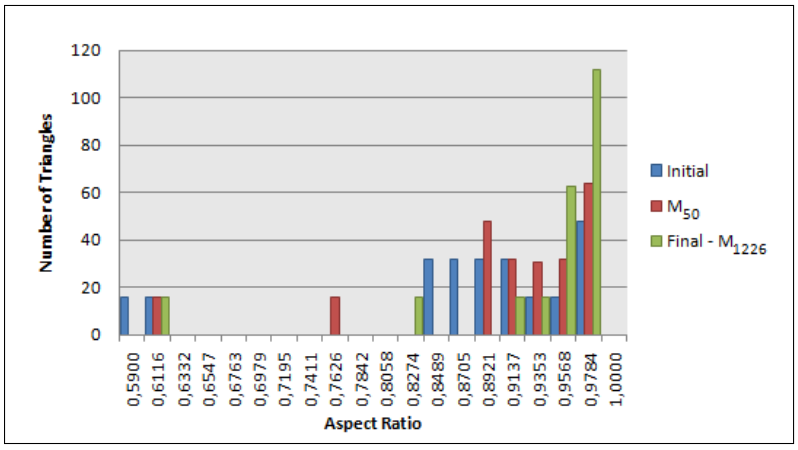


Figure 4.11: *Histogram of the triangles aspect ratio of the surfaces obtained by minimization of $E_3$ over a semi-sphere, shown in Figure 4.10.*

As in previous results, a graphic with mean, maximum and minimum of the aspect ratio triangles of the surface obtained in each iteration of the steepest descent method is presented in Figure 4.12.

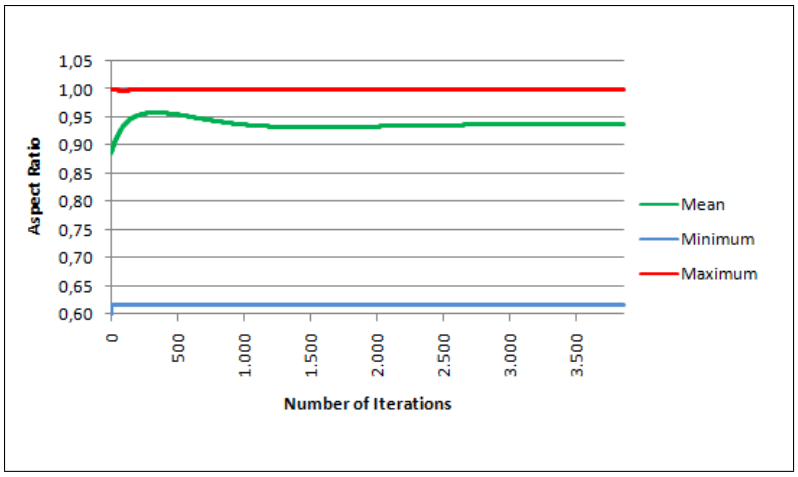


Figure 4.12: *Graphic of the mean, minimum and maximum triangles aspect ratio of the each iteration of the minimation of $E_3$ over a semi-sphere, shown in Figure 4.10.*

*Result 4:*

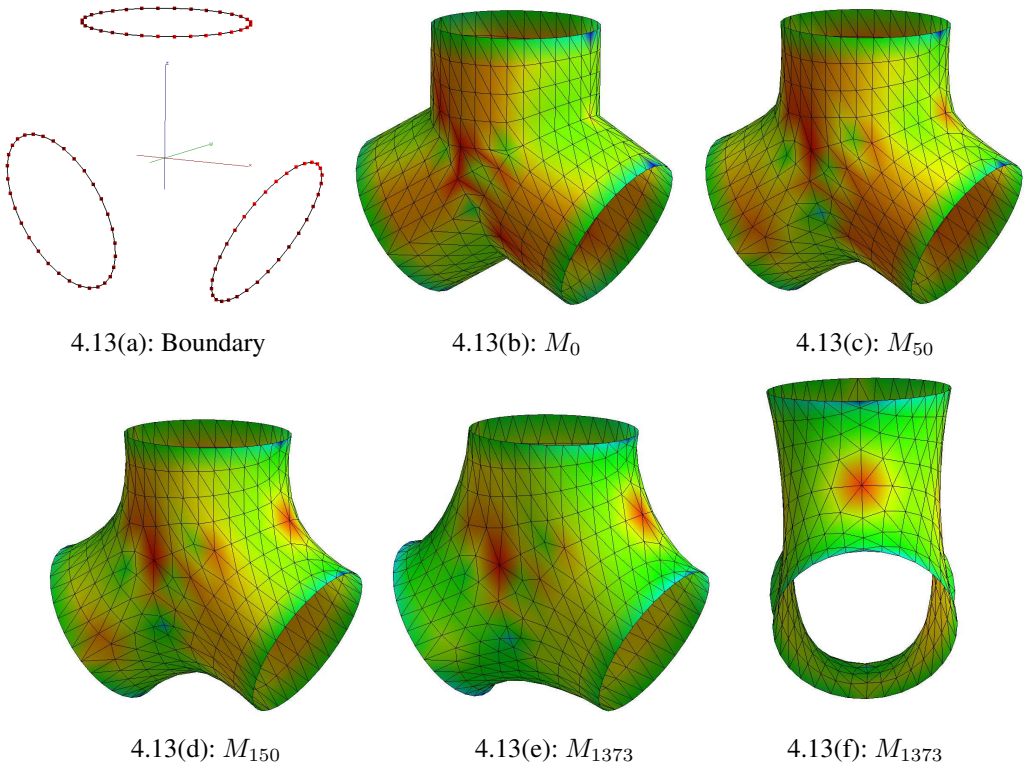

4.13(a): Boundary 4.13(b): $M_0$ 4.13(c): $M_{50}$

4.13(d): $M_{150}$ 4.13(e): $M_{1373}$ 4.13(f): $M_{1373}$

Figure 4.13: *Minimization of $E_3$ over a triangulated surface 4.13(b).*

The next result shows again the interest of energy $E_3$, since it does not create degenerate triangles during the minimization procedure and it improves the triangulation, making triangles as equilateral as possible.

$E_3$ will be minimized over the same discrete surface used in result 4 (Figure 3.5), of Chapter 3. In that minimization of $E_1$, degenerate triangles did not allow to get the desired discrete trinoid.

In Figure 4.13(a) we see the fixed boundary with $96$ vertices and Figure 4.13(b) shows the used initial approximation with $451$ vertices. In this surface there are several thin triangles, which are not so good for minimization. However, in few steps the thin triangles disappeared, see Figures 4.13(c) and 4.13(d), and the initial mesh converges to a discrete surface similar to discrete trinoid, as we can see in Figure 4.13(e). The last surface has no degeneracy, differently from the case presented in Figure 3.5.

To show the improvement of the quality of triangles in this minimization, we have a histogram with the triangles aspect ratio in some iterations of the minimization procedure. The horizontal axis is used to the value of the aspect ratio and the vertical axis, to the number of the triangles. The blue rectangle represents the initial cylinder (4.13(b)), the red rectangles represent the surface obtained after $150$ iterations of the steepest descent and finally, the green rectangles represent the

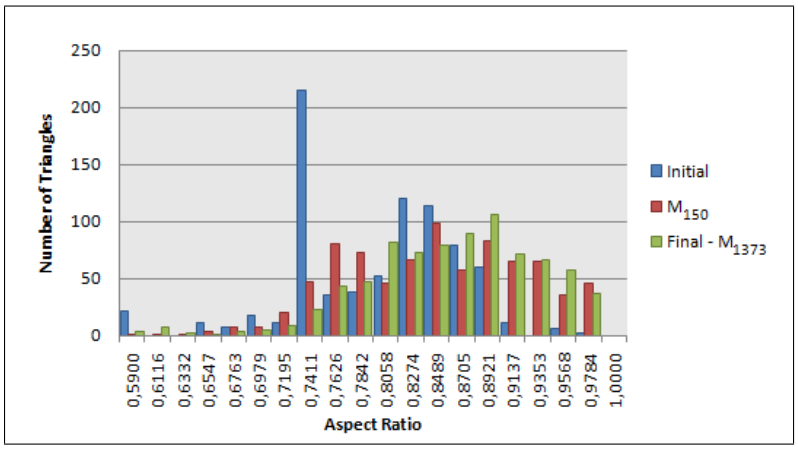


Figure 4.14: *Histogram of the triangles aspect ratio of the surfaces obtained by minimization of $E_3$ over a triangulated surface 4.13(b), shown in Figure 4.10.*

final surface obtained after 1373 iterations, shown in Figure 4.13(e). As in previous result, we see a good concentration of triangles close to aspect ratio 1 of the final surface, showing the expecting.

Once again, we show in Figure 4.15 a graphic with mean, maximum and minimum of the triangles aspect ratio in each iteration of this procedure.

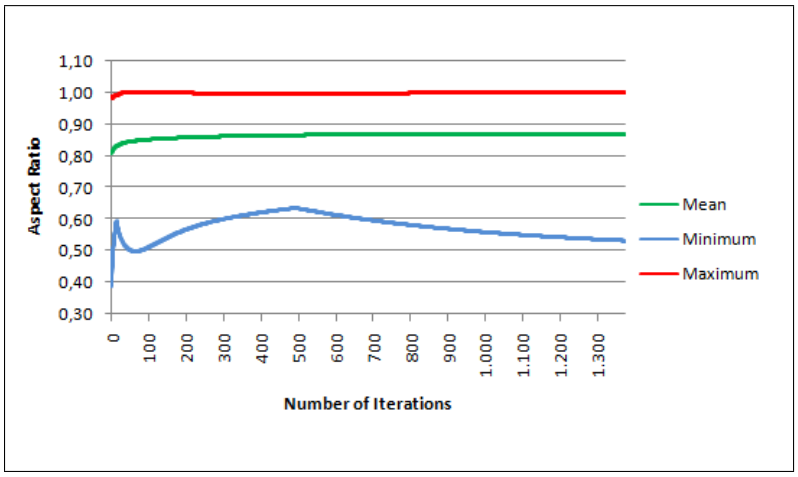


Figure 4.15: *Graphic of the mean, minimum and maximum triangles aspect ratio of the each iteration of the minimization of $E_3$ over a triangulated surface 4.13(b), shown in Figure 4.13.*

## 4.2 Properties of locally supported geometric energies

In this section we present some properties of additive locally supported geometric energies.

Remember that

$$E(M) = \sum_{T \in M} F(a, b, c)$$

where $a, b, c$ are the length of the sides of $T$ (see Figure 4.16).

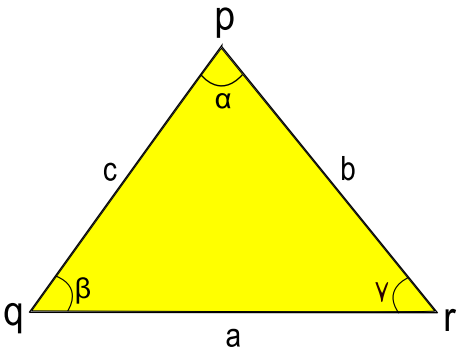


Figure 4.16: *Triangle $T$ in a triangulated surface $M$ with vertices $p, q, r$ and sides $a, b, c$.*

Observe that a triangle is determined by 3 sides, or 2 sides and 1 angle, or 2 angles and 1 side, so we can write $F(a, b, c)$ as $F(a, b, \gamma)$ or $F(a, \beta, \gamma)$.

In this subsection we shall calculate the gradient of a geometric energy. For this, we need the following lemma.

**Lemma 7** *The gradient of the angles of the triangle $T$ as in Figure 4.16 are given by:*

(1)
$$\nabla_p \gamma = \frac{\cot\alpha + \cot\gamma}{|p-r|^2}(p-q) - \frac{\cot\alpha}{|p-r|^2}(p-r), \tag{4-2}$$

(2)
$$\nabla_p \beta = \frac{-\cot\alpha}{|p-q|^2}(p-q) + \frac{\cot\alpha + \cot\beta}{|p-q|^2}(p-r), \tag{4-3}$$

(3)
$$\begin{aligned} \nabla_p \alpha &= \left( -\frac{\cot\alpha + \cot\gamma}{|p-r|^2} + \frac{\cot\alpha}{|p-q|^2} \right)(p-q) \\ &+ \left( \frac{\cot\alpha}{|p-r|^2} - \frac{\cot\alpha + \cot\beta}{|p-q|^2} \right)(p-r). \end{aligned} \tag{4-4}$$

*Proof*:

Let $J$ the rotation of $90^o$ in the plane of each triangle around $p$. We know that

$$J(e_{pq}) = -\cot\alpha(p-q) + \frac{\sin\gamma}{\sin\alpha\sin\beta}(p-r),$$

where

$$\begin{aligned} \frac{\sin\gamma}{\sin\alpha\sin\beta} &= \frac{\sin(\beta+\alpha)}{\sin\alpha\sin\beta} \\ &= \frac{\sin\beta\cos\alpha + \sin\alpha\cos\beta}{\sin\alpha\sin\beta} \\ &= \cot\alpha + \cot\beta, \end{aligned}$$

so,

$$J(e_{pq}) = -\cot\alpha(p-q) + (\cot\alpha + \cot\beta)(p-r). \tag{4-5}$$

Analogously,

$$J(e_{pr}) = \frac{-\sin\beta}{\sin\alpha\sin\gamma}(p-q) + \cot\alpha(p-r),$$

where

$$\begin{aligned}\frac{\sin\beta}{\sin\alpha\sin\gamma} &= \frac{\sin(\gamma+\alpha)}{\sin\alpha\sin\gamma} \\ &= \frac{\sin\gamma\cos\alpha + \sin\alpha\cos\gamma}{\sin\alpha\sin\gamma} \\ &= \cot\alpha + \cot\gamma,\end{aligned}$$

so,

$$J(e_{pr}) = -(\cot\alpha + \cot\gamma)(p-q) + \cot\alpha(p-r). \tag{4-6}$$

Note that the gradient of $\gamma$ is perpendicular to edge $e_{pr}$ and it must have length $\frac{1}{b}$. Analogously, the gradient of $\beta$ is perpendicular to edge $e_{pq}$ with length $\frac{1}{c}$. Then, using Equations 4-5 and 4-6, we find:

$$\begin{aligned}\nabla_p\gamma &= \frac{-J(e_{pr})}{|p-r|^2} \\ &= \frac{\cot\alpha + \cot\gamma}{|p-r|^2}(p-q) - \frac{\cot\alpha}{|p-r|^2}(p-r),\end{aligned}$$

and

$$\begin{aligned}\nabla_p\beta &= \frac{J(e_{pq})}{|p-q|^2} \\ &= \frac{-\cot\alpha}{|p-q|^2}(p-q) + \frac{\cot\alpha + \cot\beta}{|p-q|^2}(p-r).\end{aligned}$$

Besides that,

$$\alpha = \pi - \beta - \gamma,$$

it follows

$$\nabla_p\alpha = -\nabla_p\beta - \nabla_p\gamma.$$

Replacing 4-2 e 4-3 in the expression above, we get the result. ■

**Proposition 8** *The gradient of geometric energy $E$ is:*

$$\nabla_p E(M) = \sum_{t_{pqr}\in T(p)} \omega_{pq}(p-q) + \omega_{rp}(p-r), \tag{4-7}$$

*where $\omega_{pq}, \omega_{rp}$ are weights associated to edges $e_{pq}$ and $e_{rp}$ of the triangle $T$.*

*Proof*:

Let $E$ a geometric energy. We can write $E$ as follows:

$$E(M) = \sum_{T \in M} f(\alpha, \beta, a)a^2, \tag{4-8}$$

where $T$ is the triangle of the Figure 4.16.

Differentiating $E$, we find:

$$\nabla_p E(M) = \sum_{t_{pqr} \in T(p)} a^2 \left( \frac{\partial f}{\partial \alpha} \nabla_p \alpha + \frac{\partial f}{\partial \beta} \nabla_p \beta + \frac{\partial f}{\partial a} \underbrace{\nabla_p a}_{=0} \right).$$

Since

$$\alpha = \pi - \beta - \gamma,$$

thus

$$\nabla_p \alpha = -\nabla_p \beta - \nabla_p \gamma,$$

and

$$\nabla_p E(M) = \sum_{t_{pqr} \in T(p)} a^2 \left[ \left( \frac{\partial f}{\partial \beta} - \frac{\partial f}{\partial \alpha} \right) \nabla_p \beta - \frac{\partial f}{\partial \alpha} \nabla_p \gamma \right].$$

Using Equations 4-4 and 4-3, the equation above becomes:

$$\begin{aligned} \nabla_p E(M) = \sum_{t_{pqr} \in T(p)} & \left( \frac{\partial f}{\partial \beta} - \frac{\partial f}{\partial \alpha} \right) \left( \frac{-\cos \alpha}{\sin \alpha} (p - q) + \frac{\sin \gamma}{\sin \alpha \sin \beta} (p - r) \right) \frac{a^2}{c^2} \\ - & \quad \frac{\partial f}{\partial \alpha} \left( \frac{\sin \beta}{\sin \alpha \sin \gamma} (p - q) - \frac{\cos \alpha}{\sin \alpha} (p - r) \right) \frac{a^2}{b^2}. \end{aligned}$$

By the law of sines

$$\frac{a}{c} = \frac{\sin \alpha}{\sin \gamma}$$

$$\frac{a}{b} = \frac{\sin \alpha}{\sin \beta}$$

so,

$$\begin{aligned} \nabla_p E(M) = \sum_{t_{pqr} \in T(p)} & \left( - \frac{\sin^2 \alpha \cos \beta}{\sin^2 \gamma \sin \beta} \frac{\partial f}{\partial \alpha} - \frac{\sin \alpha \cos \alpha}{\sin^2 \gamma} \frac{\partial f}{\partial \beta} \right) (p - q) \\ + & \quad \left( - \frac{\sin^2 \alpha \cos \alpha}{\sin \gamma \sin^2 \beta} \frac{\partial f}{\partial \alpha} + \frac{\sin \alpha}{\sin \gamma \sin \beta} \frac{\partial f}{\partial \beta} \right) (p - r). \end{aligned}$$

As a conclusion,

$$\omega_{pq} = - \frac{\sin^2 \alpha \cos \beta}{\sin^2 \gamma \sin \beta} \frac{\partial f}{\partial \alpha} - \frac{\sin \alpha \cos \alpha}{\sin^2 \gamma} \frac{\partial f}{\partial \beta}$$

$$\omega_{rp} = -\frac{\sin^2\alpha\cos\alpha}{\sin\gamma\sin^2\beta}\frac{\partial f}{\partial\alpha} + \frac{\sin\alpha}{\sin\gamma\sin\beta}\frac{\partial f}{\partial\beta},$$

and we get the desired equations. ■

*Remark:* It is possible to prove the previous proposition writing the geometric energy $E$ as

$$E(M) = \sum_{T\in M} F(a,b,c),$$

where $T$ is the triangle of the Figure 4.16. In this case, we have

$$\omega_{pq} = \frac{1}{c}\frac{\partial F}{\partial c} \text{ and } \omega_{rp} = \frac{1}{b}\frac{\partial F}{\partial b}. \tag{4-9}$$

The gradient of the geometric energy $E$ with respect to vertex $p$ in each triangle $T = (p,q,r)$, distributes weights over the adjacent edges of $p$, given by $\omega_{pq}$ and $\omega_{rp}$. This shows that a geometric energy determines a discrete Laplacian.

From the above proposition, one easily shows that the gradient of $E_3$ is

$$\nabla_p E_3(M) = \sum_{t_{pqr}\in T(p)} \left(\frac{\cot\alpha\cot\beta}{2\sin^2\gamma}\right)(p-q) + \left(\frac{\cot\alpha\cot\gamma}{2\sin^2\beta}\right)(p-r),$$

where $T$ is the triangle of the Figure 4.16.

## 4.3 Discrete Laplacians

In this section, we will define the discrete Laplacian and present some properties analogous to those of the smooth Laplacian.

**Definition 9** *A general discrete Laplacian is defined at a vertex $p \in M$ by*

$$L(p) = \sum_{q\in N(p)} \omega_{pq}(p-q), \tag{4-10}$$

*where $\omega_{pq}$ are the weights of the edges.*

*The $n \times n$ Laplacian matrix $L$ of $M$ and its coordinates $l_{pq}$ are given by:*

$$l_{pq} = \begin{cases} -\omega_{pq}, & \text{if} \quad p \neq q \\ \displaystyle\sum_{q\in N(p)} \omega_{pq}, & \text{if} \quad p = q. \end{cases}$$

We describe a set of properties of discrete Laplacians following (34):

1. Symmetry: the discrete Laplacian is symmetric if

$$\omega_{pq} = \omega_{qp},$$

over all $p \neq q$.

2. Local support: weights are associated to mesh edges, so

$$\omega_{pq} = 0, \text{ if } p \text{ and } q \text{ do not share a edge.}$$

We include in this definition the property that $\omega_{pq}$ depends only on the triangles adjacent to $e_{pq}$, although this property was not mentioned in (34).

3. Positivity: this property is satisfied if

$$\omega_{pq} > 0$$

over all $p \neq q$. With this property, it is possible to establish a connection to barycentric coordinates by setting

$$\lambda_{pq} = \frac{\omega_{pq}}{\sum_{p \neq q} \omega_{pq}} \Rightarrow \sum_{p \neq q} \lambda_{pq} = 1.$$

These properties can be satisfied or not by a Laplacian. Other properties can be found in (34).

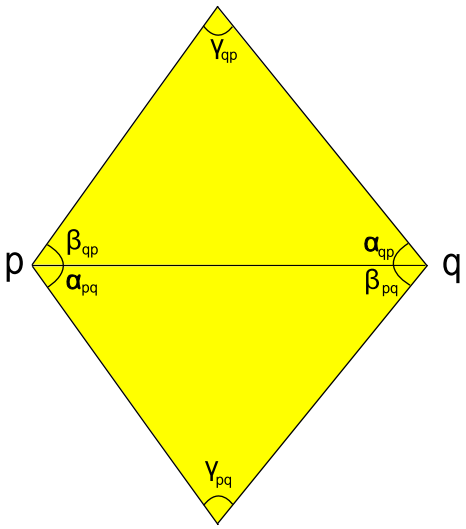


Figure 4.17: *Angles used in discrete Laplacian examples.*

In the following, we enumerate known discrete Laplacians, all satisfying the local support property:

1. Combinatorial Laplacian: $\omega_{pq} = 1$ (cited in Subsection 4.1.2). Observe that this Laplacian is symmetric and positive.

2. Tutte Laplacian: $\omega_{pq} = \frac{1}{d_p}$ (cited in Subsection 4.1.2). Observe that this Laplacian is positive, but not symmetric.

3. Cotangents Laplacian: $\omega_{pq} = \cot\gamma_{pq} + \cot\gamma_{qp}$, where $\gamma_{pq}, \gamma_{qp}$ are in Figure 4.17 (cited in Chapter 3). Observe that this Laplacian is symmetric, but not positive.

4. Wachspress Laplacian: $\omega_{pq} = \dfrac{\cot\alpha_{qp} + \cot\beta_{pq}}{|p-q|^2}$, where $\beta_{pq}, \alpha_{qp}$ are in the Figure 4.17. Observe that this Laplacian is not symmetric and not positive. In (33), this Laplacian is used to parametrize discrete surfaces.

5. Mean value Laplacian: $\omega_{pq} = \dfrac{\tan\frac{\alpha_{pq}}{2} + \tan\frac{\beta_{pq}}{2}}{|p-q|}$, where $\alpha_{pq}, \beta_{qp}$ are in the Figure 4.17. Observe that this Laplacian is not symmetric and not positive. In (11), this Laplacian is also used to parametrize discrete surfaces.



## 4.4
## Discrete Laplacians from geometric energies

We have observed that the gradient of a geometric energy defines a locally supported discrete Laplacian. In this section we characterize the discrete Laplacian that comes from locally supported geometric energies.

### 4.4.1
### Symmetry of Laplacians coming from geometric energies

We say that a discrete Laplacian comes from a geometric energy $E$ if

$$L(p) = \nabla_p E,$$

for all $p \in M$.

Immediately we observe that $L$ satisfies local support property, since geometric energies satisfy this property.

In the following, we prove that discrete Laplacians coming from geometric energies are symmetric.

**Theorem 10** *Discrete Laplacians coming from geometric energies are symmetric.*

*Proof*:

In Section 4.2, we have proved that

$$\nabla_p E(M) = \sum_{T \in T(p)} \omega_{pq}(p-q) + \omega_{pr}(p-r)$$

where $T$ is given in Figure 4.16.

To simplify, we will consider only the contribution of the triangle $T$ to $\nabla_p E(M)$ given by

$$\omega_{pq}(p-q)+\omega_{pr}(p-r),$$

where,

$$\omega_{pq}=-\frac{\sin^2\alpha\cos\beta}{\sin^2\gamma\sin\beta}\frac{\partial f}{\partial\alpha}-\frac{\sin\alpha\cos\alpha}{\sin^2\gamma}\frac{\partial f}{\partial\beta}$$

$$\omega_{pr}=-\frac{\sin^2\alpha\cos\alpha}{\sin\gamma\sin^2\beta}\frac{\partial f}{\partial\alpha}+\frac{\sin\alpha}{\sin\gamma\sin\beta}\frac{\partial f}{\partial\beta}.$$

In order to prove that $L$ is symmetric, we need to compare $\omega_{pq}$ and $\omega_{qp}$. To calculate $\omega_{qp}$, we use the following equation to a geometric energy $E$

$$E(M)=\sum_{T\in M} g(\alpha,\beta,b)b^2.$$

The contribution of the triangle $T$ to $\nabla_q E(M)$ is

$$\omega_{qp}(q-p)+\omega_{qr}(q-r),$$

where

$$\omega_{qp}=-\frac{\sin^2\beta\cos\alpha}{\sin\alpha\sin^2\gamma}\frac{\partial g}{\partial\beta}-\frac{\sin\beta\cos\beta}{\sin^2\gamma}\frac{\partial g}{\partial\alpha}$$

$$\omega_{qr}=-\frac{\sin^2\beta\cos\gamma}{\sin\gamma\sin^2\alpha}\frac{\partial g}{\partial\beta}+\frac{\sin\beta}{\sin\alpha\sin\gamma}\frac{\partial g}{\partial\alpha}.$$

*Claim:* $\omega_{pq}=\omega_{qp}$.

To calculate $\omega_{pq}$, previously we use Equation 4-8 with function $f(\alpha,\beta,a)$. To compute $\omega_{qp}$, we use the function $g(\alpha,\beta,b)$ in definition of $E$, given above. By the law of sines

$$a=\frac{\sin\alpha}{\sin\beta}b,$$

thus $a=a(\alpha,\beta,b)$, and

$$f(\alpha,\beta,a)a^2=f\big(\alpha,\beta,a(\alpha,\beta,b)\big)\frac{\sin^2\alpha}{\sin^2\beta}b^2.$$

So

$$g(\alpha,\beta,b)=f\big(\alpha,\beta,a\big)\frac{\sin^2\alpha}{\sin^2\beta},$$

that implies,

$$\frac{\partial g}{\partial\alpha}=\frac{\partial f}{\partial\alpha}\frac{\sin^2\alpha}{\sin^2\beta}+\frac{2f\sin\alpha\cos\alpha}{\sin^2\beta}+b\frac{\partial f}{\partial a}\frac{\sin^2\alpha\cos\alpha}{\sin^3\beta}.$$

$$\frac{\partial g}{\partial \beta} = \frac{\partial f}{\partial \beta}\frac{\sin^2\alpha}{\sin^2\beta} - \frac{2f\sin^2\alpha\cos\beta}{\sin^3\beta} - b\frac{\partial f}{\partial a}\frac{\sin^3\alpha\cos\beta}{\sin^4\beta}.$$

Replacing the above equations in $\omega_{qp}$, we get

$$\omega_{qp} = \omega_{pq}.$$

■

*Remark:* The previous theorem is immediate if $E$ is written as

$$E(M) = \sum_{T\in M} F(a,b,c)$$

and the gradient

$$\nabla_p E(M) = \sum_{t_{pqr}T(p)} \omega_{pq}(p-q) + \omega_{rp}(p-r)$$

where $\omega_{pq}$ and $\omega_{rp}$ are given by Equation 4-9, since the $\omega_{pq}$ and $\omega_{rp}$ depends only on $b$ and $c$, the adjacent sides to $e_{pq}$.

With this theorem we conclude that if a discrete Laplacian does not satisfy the symmetry property, it can not come from some geometric energy. Symmetry is a necessary condition for Laplacian to come from geometric energies, but it is not a sufficient condition. In next subsection, we examine a sufficient condition.

It follows from this theorem that the Tutte Laplacian, the Wachspress Laplacian and the Mean value Laplacian do not come from geometric energies (see Section 4.3).

### 4.4.2 Conditions for a symmetric Laplacian to come from a geometric energy

In this subsection we analyze the sufficient condition for a discrete symmetric Laplacian $L$ to come from an additive locally supported geometric energy $E$.

Let $L$ be a discrete symmetric Laplacian defined on a discrete surface $M$ with triangles $T$, as in Figure 4.16. Let **F** be the field defined by the Laplacian $L$ in the plane of a triangle $T$ in $M$, i.e., we will consider only the weights of the edges of the triangle $T$ and

$$\mathbf{F}(p) = \omega_0(\alpha,\beta,|e_{qr}|)(p-q) + \omega_1(\alpha,\beta,|e_{qr}|)(p-r).$$

If $L$ comes from an energy then **F** must be conservative.

Assume $q = (0, 0)$ and $r = (t, 0)$ are fixed, and $p = (x, y)$. Then

$$\begin{aligned} \mathbf{F}(x, y) &= \omega_0(p - q) + \omega_1(p - r) \\ &= (x\omega_0 + (x - t)\omega_1, y\omega_0 + y\omega_1) \end{aligned}$$

where $t$ is the length of $e_{qr}$.

**Lemma 11** *Assume that $L$ comes from an energy. Then,*

$$\begin{aligned} &\frac{\partial \omega_0}{\partial \alpha}(\sin\gamma \sin\alpha \cos\gamma) + \frac{\partial \omega_0}{\partial \beta}(-\sin\beta \sin\gamma) = \\ &\frac{\partial \omega_1}{\partial \alpha}(\sin\beta \sin\alpha \cos\beta) + \frac{\partial \omega_1}{\partial \beta}(\sin^2\beta \cos\alpha). \end{aligned} \tag{4-11}$$

*Proof*:

If $\mathbf{F}$ comes from a geometric energy $E$, then $\mathbf{F}$ is conservative. This implies that

$$y\left(\frac{\partial \omega_0}{\partial x} + \frac{\partial \omega_1}{\partial x}\right) = x\frac{\partial \omega_0}{\partial y} + (x - t)\frac{\partial \omega_1}{\partial y}. \tag{4-12}$$

By making a change of variables

$$\begin{aligned} x(\alpha, \beta) &= t\frac{\sin\gamma \cos\beta}{\sin\alpha} \\ y(\alpha, \beta) &= t\frac{\sin\gamma \sin\beta}{\sin\alpha} \\ x(\alpha, \beta) - t &= t\frac{\sin\beta \cos\gamma}{\sin\alpha}, \end{aligned}$$

it follows that

$$\begin{aligned} \frac{\partial x(\alpha, \beta)}{\partial \beta} &= -t\left(\frac{\cos\beta \cos\gamma + \sin\beta \sin\gamma}{\sin\alpha}\right) \\ \frac{\partial x(\alpha, \beta)}{\partial \alpha} &= -t\frac{\sin\beta \cos\beta}{\sin^2\alpha} \\ \frac{\partial y(\alpha, \beta)}{\partial \beta} &= -t\left(\frac{\sin\beta \cos\gamma - \sin\gamma \cos\beta}{\sin\alpha}\right) \\ \frac{\partial y(\alpha, \beta)}{\partial \alpha} &= -t\frac{\sin^2\beta}{\sin^2\alpha}. \end{aligned}$$

With the equations

$$\begin{aligned} \frac{\partial \omega_i}{\partial \beta} &= \frac{\partial \omega_i}{\partial x}\frac{\partial x}{\partial \beta} + \frac{\partial \omega_i}{\partial y}\frac{\partial y}{\partial \beta} \\ \frac{\partial \omega_i}{\partial \alpha} &= \frac{\partial \omega_i}{\partial x}\frac{\partial x}{\partial \alpha} + \frac{\partial \omega_i}{\partial y}\frac{\partial y}{\partial \alpha} \end{aligned}$$

for $i = 0, 1$, equation 4-11 becomes

$$\begin{aligned} t \quad & \frac{\sin^2\gamma\sin^2\beta}{\sin\alpha}\frac{\partial\omega_0}{\partial x} - t\frac{\sin^2\gamma\sin\beta\cos\beta}{\sin\alpha}\frac{\partial\omega_0}{\partial y} = \\ t \quad & \left(\frac{-\sin^2\beta\cos^2\beta - \sin^2\beta\cos\gamma\cos\beta\cos\alpha - \sin\gamma\sin^3\beta\cos\alpha}{\sin\alpha}\right)\frac{\partial\omega_1}{\partial x} + \\ t \quad & \left(\frac{-\sin^3\beta\cos\beta - \sin^3\beta\cos\gamma\cos\alpha + \sin\gamma\sin^2\beta\cos\beta\cos\alpha}{\sin\alpha}\right)\frac{\partial\omega_1}{\partial y}. \end{aligned}$$

Simplifying, we get

$$t\frac{\sin\gamma\sin\beta}{\sin\alpha}\frac{\partial\omega_0}{\partial x} - t\frac{\sin\gamma\cos\beta}{\sin\alpha}\frac{\partial\omega_0}{\partial y} = -t\frac{\sin\gamma\sin\beta}{\sin\alpha}\frac{\partial\omega_1}{\partial x} - t\frac{\sin\beta\cos\gamma}{\sin\alpha}\frac{\partial\omega_1}{\partial y},$$

and replacing $x, y, x - t$, the equation above reduces to 4-12. ■

The condition obtained in previous lemma can be written in another way to provide a symmetric equation. For this, we can change variables:

$$\omega_i(\alpha, \beta) = \omega_i(\beta, \pi - \alpha - \beta),$$

where $i = 0, 1$. In this case we have,

$$\frac{\partial\omega_i}{\partial\alpha} = \frac{\partial\omega_i}{\partial\beta}\frac{\partial\beta}{\partial\alpha} + \frac{\partial\omega_i}{\partial\gamma}\frac{\partial\gamma}{\partial\alpha} = -\frac{\partial\omega_i}{\partial\gamma}$$

$$\frac{\partial\omega_i}{\partial\beta} = \frac{\partial\omega_i}{\partial\beta}\frac{\partial\beta}{\partial\beta} + \frac{\partial\omega_i}{\partial\gamma}\frac{\partial\gamma}{\partial\beta} = \frac{\partial\omega_i}{\partial\beta} - \frac{\partial\omega_i}{\partial\gamma},$$

and replacing in 4-11 we find:

$$\begin{aligned} & \frac{\partial\omega_0}{\partial\gamma}(\sin^2\gamma\cos\alpha) - \frac{\partial\omega_0}{\partial\beta}(\sin\beta\sin\gamma) = \\ & \frac{\partial\omega_1}{\partial\beta}(\sin^2\beta\cos\alpha) - \frac{\partial\omega_1}{\partial\gamma}(\sin\beta\sin\gamma). \end{aligned} \tag{4-13}$$

The next theorem shows that Equation 4-13 is also sufficient for a Laplacian to come from a geometric energy.

**Theorem 12** *If condition 4-13 is satisfied for any pairs of adjacent edges, then $L$ comes from a geometric energy $E$.*

In the remainder of the subsection, we present the proof of this theorem. First we need a lemma. Let

$$u_0 = \frac{p - q}{|p - q|^2}$$

$$u_1 = \frac{p - r}{|p - r|^2}$$

$$u_2 = \frac{q-r}{|q-r|^2}.$$

**Lemma 13** *Considering the contribution of the triangle $T$, given by Figure 4.16, to $L(p)$ and $L(q)$, we have*

$$\nabla_q L(p) = \bar{a}u_1u_1^t + \bar{b}u_1u_2^t + \bar{c}u_2u_1^t + \bar{d}u_2u_2^t - \omega_0 I,$$

*where*

$$\begin{aligned}
\bar{a} &= \bar{A}\frac{\sin^2\beta}{\sin^2\gamma} + \bar{B}\frac{\sin\beta\sin\alpha}{\sin^2\gamma} \\
\bar{b} &= -\bar{A}\frac{\sin\beta\sin\alpha}{\sin^2\gamma} \\
\bar{c} &= -\bar{A}\frac{\sin\beta\sin\alpha}{\sin^2\gamma} - \bar{B}\frac{\sin\alpha}{\sin\gamma} + \bar{C}\frac{\sin\beta}{\sin\gamma} + \bar{D} \\
\bar{d} &= \bar{A}\frac{\sin^2\alpha}{\sin^2\gamma} - \bar{C}\frac{\sin\alpha}{\sin\gamma}
\end{aligned} \tag{4-14}$$

*and*

$$\begin{aligned}
\bar{A} &= \frac{\partial\omega_0}{\partial\alpha}\frac{\cos\beta}{\sin\beta} + \frac{\partial\omega_0}{\partial\beta}\frac{\cos\alpha}{\sin\alpha} + \frac{\partial\omega_0}{\partial c}c \\
\bar{B} &= \frac{\partial\omega_1}{\partial\alpha}\frac{\cos\beta}{\sin\gamma} + \frac{\partial\omega_1}{\partial\beta}\frac{\sin\beta\cos\alpha}{\sin\alpha\sin\gamma} \\
\bar{C} &= \frac{\partial\omega_0}{\partial\alpha}\frac{1}{\sin\beta} - \frac{\partial\omega_0}{\partial\beta}\frac{\cos\gamma}{\sin\alpha} \\
\bar{D} &= \frac{\partial\omega_1}{\partial\alpha}\frac{1}{\sin\gamma} - \frac{\partial\omega_1}{\partial\beta}\frac{\sin\beta\cos\gamma}{\sin\alpha\sin\gamma}.
\end{aligned}$$

*Moreover,*

$$\nabla_p L(q) = \bar{e}u_1u_1^t + \bar{f}u_1u_2^t + \bar{g}u_2u_1^t + \bar{h}u_2u_2^t - \omega_0 I,$$

*where*

$$\begin{aligned}
\bar{e} &= \bar{E}\frac{\sin^2\beta}{\sin^2\gamma} + \bar{F}\frac{\sin\beta}{\sin\gamma} \\
\bar{f} &= -\bar{E}\frac{\sin\beta\sin\alpha}{\sin^2\gamma} + \bar{G}\frac{\sin\beta}{\sin\gamma} - \bar{F}\frac{\sin\alpha}{\sin\gamma} + \bar{H} \\
\bar{g} &= -\bar{E}\frac{\sin\beta\sin\alpha}{\sin^2\gamma} \\
\bar{h} &= \bar{E}\frac{\sin^2\alpha}{\sin^2\gamma} - \bar{G}\frac{\sin\alpha}{\sin\gamma}
\end{aligned} \tag{4-15}$$

*and,*

$$\begin{aligned}
\bar{E} &= \frac{\partial\omega_0}{\partial\alpha}\frac{\cos\beta}{\sin\beta} + \frac{\partial\omega_0}{\partial\beta}\frac{\cos\alpha}{\sin\alpha} + \frac{\partial\omega_0}{\partial c}\frac{1}{c} \\
\bar{F} &= \frac{\partial\omega_0}{\partial\alpha}\frac{\cos\gamma}{\sin\beta} - \frac{\partial\omega_0}{\partial\beta}\frac{1}{\sin\alpha} \\
\bar{G} &= -\frac{\partial\omega_2}{\partial\alpha}\frac{\sin\alpha\cos\beta}{\sin\gamma\sin\beta} - \frac{\partial\omega_2}{\partial\beta}\frac{\cos\alpha}{\sin\gamma} \\
\bar{H} &= -\frac{\partial\omega_2}{\partial\alpha}\frac{\sin\alpha\cos\gamma}{\sin\gamma\sin\beta} + \frac{\partial\omega_2}{\partial\beta}\frac{1}{\sin\gamma}
\end{aligned}$$

*and $I$ represents the $3 \times 3$ identity matrix.*

*Proof*:

Write

$$L(p) = \omega_0(p-q) + \omega_1(p-r),$$

$$L(q) = \omega_0(q-p) + \omega_2(q-r),$$

where $\omega_0, \omega_1, \omega_2$ are the weights of the edges $e_{pq}, e_{qr}, e_{rp}$ of the triangle $T$. Without loss of generality, we consider

$$\omega_0 = \omega_0(\beta, \alpha, c),$$

$$\omega_1 = \omega_1(\beta, \alpha, b),$$

$$\omega_2 = \omega_2(\beta, \alpha, a),$$

since $E$, by definition, can be computed in many ways and consequently its gradient.

Differentiating $L(p)$ we obtain

$$\begin{aligned}
\nabla_q L(p) &= \nabla_q\omega_0(p-q)^t + \nabla_q\omega_1(p-r)^t - \omega_0 I \\
&= \left(\frac{\partial\omega_0}{\partial\alpha}\nabla_q\alpha + \frac{\partial\omega_0}{\partial\beta}\nabla_q\beta + \frac{\partial\omega_0}{\partial c}\nabla_q c\right)(p-q)^t \\
&+ \left(\frac{\partial\omega_1}{\partial\alpha}\nabla_q\alpha + \frac{\partial\omega_1}{\partial\beta}\nabla_q\beta + \frac{\partial\omega_1}{\partial b}\nabla_q b\right)(p-r)^t - \omega_0 I.
\end{aligned} \tag{4-16}$$

From analogous computations to 4-4 and 4-3 we get:

$$\begin{aligned}
\nabla_q \alpha(p-q)^t &= \left(\frac{\cos\beta}{\sin\beta}\right) u_0 u_0^t + \left(\frac{1}{\sin\beta}\right) u_2 u_0^t \\
\nabla_q \alpha(p-r)^t &= \left(\frac{\cos\beta}{\sin\gamma}\right) u_0 u_1^t + \left(\frac{1}{\sin\gamma}\right) u_2 u_1^t \\
\nabla_q \beta(p-r)^t &= \left(\frac{\sin\beta\cos\alpha}{\sin\alpha\sin\gamma}\right) u_0 u_1^t - \left(\frac{\sin\beta\cos\gamma}{\sin\alpha\sin\gamma}\right) u_2 u_1^t \\
\nabla_q \beta(p-q)^t &= \left(\frac{\cos\alpha}{\sin\alpha}\right) u_0 u_0^t - \left(\frac{\cos\gamma}{\sin\alpha}\right) u_2 u_0^t, \\
\nabla_q c(p-q)^t &= c u_0 u_0^t
\end{aligned}$$

and replacing in 4-16 follows:

$$\nabla_q L(p) = \bar{A} u_0 u_0^t + \bar{B} u_0 u_1^t + \bar{C} u_2 u_0^t + \bar{D} u_2 u_1^t - \omega_0 I,$$

where

$$\begin{aligned}
\bar{A} &= \frac{\partial\omega_0}{\partial\alpha}\frac{\cos\beta}{\sin\beta} + \frac{\partial\omega_0}{\partial\beta}\frac{\cos\alpha}{\sin\alpha} + \frac{\partial\omega_0}{\partial c}c \\
\bar{B} &= \frac{\partial\omega_1}{\partial\alpha}\frac{\cos\beta}{\sin\gamma} + \frac{\partial\omega_1}{\partial\beta}\frac{\sin\beta\cos\alpha}{\sin\alpha\sin\gamma} \\
\bar{C} &= \frac{\partial\omega_0}{\partial\alpha}\frac{1}{\sin\beta} - \frac{\partial\omega_0}{\partial\beta}\frac{\cos\gamma}{\sin\alpha} \\
\bar{D} &= \frac{\partial\omega_1}{\partial\alpha}\frac{1}{\sin\gamma} - \frac{\partial\omega_1}{\partial\beta}\frac{\sin\beta\cos\gamma}{\sin\alpha\sin\gamma}.
\end{aligned}$$

Using the following identity

$$\sin\gamma u_0 = \sin\beta u_1 - \sin\alpha u_2, \tag{4-17}$$

we get the desired equation. The other equation is obtained analogously. ■

Now we prove the theorem 12.

*Proof*:

To show that $L$ comes from a geometric energy $E$, it is sufficient that for any pair of vertices $p$ and $q$ sharing a edge

$$\nabla_q L(p) = \nabla_p L(q),$$

or equivalently,

$$\frac{\partial^2 E(M)}{\partial q \partial p} = \left(\frac{\partial^2 E(M)}{\partial p \partial q}\right)^t.$$

Using the previous lemma, the condition above can be written as

$$\bar{a} = \bar{e}$$

$$\bar{b} = \bar{g}$$

$$\bar{c} = \bar{f}$$

$$\bar{d} = \bar{h}.$$

First of all, the condition $\bar{b} = \bar{g}$ is always satisfied. Now, it is very simple to see that if 4-13 is satisfied, then $\bar{a} = \bar{e}$.

Now, we suppose that Condition 4-13 is a function of $\omega_0, \omega_1, \alpha, \beta, \gamma$. By the symmetry of the triangle, this condition is also satisfied with a permutation of arguments. For example, using $\omega_1, \omega_2, \gamma, \alpha, \beta$, Condition 4-13 becomes

$$\begin{aligned} &\frac{\partial \omega_0}{\partial \alpha}(-\sin\gamma\sin\alpha) + \frac{\partial \omega_0}{\partial \beta}(\sin\gamma\sin\beta\cos\gamma) = \\ &\frac{\partial \omega_2}{\partial \alpha}(\sin^2\alpha\cos\beta) + \frac{\partial \omega_2}{\partial \beta}(\sin\beta\sin\alpha\cos\alpha). \end{aligned} \tag{4-18}$$

Making simple calculations, we can see that if 4-18 is satisfied, then $\bar{d} = \bar{h}$. Another permutation of arguments can be done to get:

$$\begin{aligned} &\frac{\partial \omega_1}{\partial \alpha}(\sin\beta\sin\alpha) - \frac{\partial \omega_1}{\partial \beta}(\sin^2\beta\cos\gamma) = \\ &-\frac{\partial \omega_2}{\partial \alpha}(\sin^2\alpha\cos\gamma) + \frac{\partial \omega_2}{\partial \beta}(\sin\beta\sin\alpha). \end{aligned} \tag{4-19}$$

It follows that if 4-19 is satisfied, then we get $\bar{c} = \bar{f}$, which proves the theorem. ■

## 4.5 Index

In this section, we will study the index of a discrete surface.

In the continuous case, the index of a minimal surface $S$ is the number of negative eigenvalues of the second variation of area, for any variation of $S$ with compact support. Analogously, in the discrete case, Polthier and Rossman in (23) computed the index of a critical point of the area functional by evaluating the number of negative eigenvalues of the area Hessian. When the index is zero, the surface is called stable, as in the continuous case.

Motivated by the index of discrete minimal surfaces, we define the index of any critical point to some geometric energy:

**Definition 14** *Let $E$ a geometric energy. The index of triangulated surface that is a critical point of $E$ is the number of negative eigenvalues of the Hessian of $E(M)$.*

In particular, if $E$ is the area functional and $M$ is a discrete minimal surface, we have the index definition cited above. Like in the continuous case, eigenvectors associated to negative eigenvalues represent the directions of variations that reduce $E$. So, if the index of critical point of a given geometric energy is 0, we conclude that the critical point is a minimum of the energy $E$.

### 4.5.1 Index associated to the area energy $E_1$

First of all, to compute index of surfaces with respect to area, it is necessary to compute the Hessian of area:

**Lemma 15** *The Hessian of the area functional from $M$ to $\mathbb{R}$ is a symmetric bilinear form with $3n \times 3n$ matrix representation $H$. $H$ can be considered as a $n \times n$ grid with $3 \times 3$ entry $H(p,q)$ for each pair of interior vertices $p$ and $q$.*

*When $p$ and $q$ are not adjacent, we have:*

$$H(p,q) = 0.$$

*If $p$ and $q$ are adjacent and unequal, we have*

$$H(p,q) = \frac{1}{2} \sum_{\substack{T=(p,q,r) \\ p,q \text{ are fixed}}} \frac{e_{pq} J^t(e_{pq}) - J^t(e_{pq}) e_{pq}^t}{|e_{pq}|^2} - \cot\theta \; NN^t$$

*where $J$ is the rotation of $90^o$, $\theta$ is the interior angle of the triangle $T = (p,q,r)$ at $r$. And finally,*

$$H(p,p) = \frac{1}{4} \sum_{T(p) \in M} \frac{|e_{rq}|^2}{\text{area } T} \; NN^t.$$

*$N$ denotes the oriented unit normal vector of the triangle $T = (p,q,r)$.*

This lemma is proved in (23).

The number of the negative eigenvalues of $H(p,p)$ will be called local index of $p$ if $p$ is an interior vertex of $M$.

With the lemma above, it is possible to compute the index of any discrete minimal surface with respect to the area, by evaluating the number of negative points in the spectrum of $H$.

In (23), Polthier et al. computed the index of discrete minimal surfaces; for example a discrete catenoid has index 1, a discrete trinoid has index 3, the Costa surface has index 5.

Now we will prove a local property of the area functional:

**Lemma 16** *(see (23)) The area functional is convex in each direction $p \in \mathbb{R}^3$.*

*Proof*:

Let $M$ a discrete surface, and $p$ a interior point of $M$. For all vectors $u \in \mathbb{R}^3$ we have:

$$\begin{aligned} uH(p,p)u^t &= u\,\frac{1}{4}\sum_{T(p)\in M}\frac{|e_{rq}|^2}{\text{area } T}NN^t\,u^t \\ &= \frac{1}{4}\sum_{T(p)\in M}\frac{|e_{rq}|^2}{\text{area } T}\,uNN^t\,u^t \\ &= \frac{1}{4}\sum_{T(p)\in M}\frac{|e_{rq}|^2}{\text{area } T} < u, N >^2 \\ &\geq 0, \end{aligned}$$

so $H(p,p)$ is a positive-definite matrix. Therefore, the area is convex in a direction $p$.

■

Therefore, by the lemma, in a discrete minimal surface, every geometric realization of a vertex with all others vertices fixed are minimal for area energy. Or equivalently, the local index with respect to area of any vertex in $M$ is 0. This is very strong property, since it is valid for any configuration in a discrete minimal surface.

### 4.5.2 Index associated to $E_2$

The geometric energy

$$E_2(M) = \sum_{e_{pq}\in Edges(M)} |e_{pq}|^2$$

has an interesting property given by the following lemma:

**Lemma 17** *The real function $E_2$ defined on a triangulated surface $M$ is a convex function.*

*Proof*:

Let $U$ the set of triangulated surfaces with $n$ vertices and the same topology. We consider

$$E_2 : U \subset \mathbb{R}^{3n} \longrightarrow \mathbb{R},$$

that is, $E_2$ is a real function defined over all coordinates of the vertices of the surface $M \in U$.

So, let $M_i, M_j \in U$

$$M_i = \{(p_1^i, p_2^i, \ldots, p_n^i), p_k^i \in \mathbb{R}^3\}$$

$$M_j = \{(p_1^j, p_2^j, \ldots, p_n^j), p_l^j \in \mathbb{R}^3\}$$

two discrete surfaces. Then,

$$\begin{aligned} E_2(\lambda M_i + (1-\lambda)M_j) &= \sum_e |(\lambda p_k^i + (1-\lambda)p_k^j) - (\lambda p_l^i + (1-\lambda)p_l^j)|^2 \\ &= \sum_e |\lambda(p_k^i - p_l^i) + (1-\lambda)(p_k^j - p_l^j)|^2 \\ &\leq \sum_e \lambda|p_k^i - p_l^i|^2 + (1-\lambda)|p_k^j - p_l^j|^2, \end{aligned}$$

for any $\lambda \in (0,1)$.

Thus, $E_2$ is a convex function. ■

With this lemma, we have proved that all triangulated surfaces that are critical point of $E_2$ are minimum to $E_2$, that is, the index of any critical point of $E_2$ is 0. In particular, the local index of all critical interior points of $M$ is also 0.

This property satisfied by $E_2$ is stronger than the property satisfied by area functional, since in the area case we proved that any discrete surface is locally convex and $E_2$ case, we proved that any critical point of $E_2$ is a minimum of $E_2$. In this context, we can ask if there are other geometric energies with these properties. But, we do not know the answer.

In the following we will compute a general Hessian of a given geometric energy $E$, and we show some results of index with respect to other energies.

### 4.5.3 Index associated to $E$

To compute the index of a discrete surface with respect to $E$, it is necessary to find the Hessian of $E$:

**Lemma 18** *Let $E$ a geometric energy from $M$ to $\mathbb{R}$ such that*

$$\nabla_p E(M) = \sum_{t_{pqr} \in T(p)} \omega_0(\alpha, \beta, c)(p-q) + \omega_1(\alpha, \beta, b)(p-r),$$

*where $T$ is a triangle as in the Figure 4.16.*

*The Hessian $E$ is a symmetric bilinear form with $3n \times 3n$ matrix representation $H$. $H$ can be considered as a $n \times n$ grid with $3 \times 3$ entry $H(p,q)$ for each pair of interior vertices $p$ and $q$. If the vertices $p$ and $q$ are not adjacent,*

$$H(p,q) = 0.$$

*If $p$ and $q$ are adjacent and unequal,*

$$H(p,q) = \sum_{\substack{T=(p,q,r) \\ p,q \text{ are fixed}}} \bar{a}u_1u_1^t + \bar{b}u_1u_2^t + \bar{c}u_2u_1^t + \bar{d}u_2u_2^t - \omega_0 I$$

*where $\bar{a}, \bar{b}, \bar{c}, \bar{d}$ are given in Equation 4-14.*

*And finally,*

$$H(p,p) = \sum_{T(p)\in M} \bar{e}u_0u_0^t + \bar{f}u_1u_0^t + \bar{g}u_0u_1^t + \bar{h}u_1u_1^t + (\omega_0 + \omega_1)I$$

*so that $I$ is the $3 \times 3$ identity matrix and*

$$\begin{aligned}
\bar{e} &= -\frac{\partial\omega_0}{\partial\alpha}\frac{\cos\beta}{\sin\beta} - \frac{\partial\omega_0}{\partial\beta}\frac{\cos\alpha}{\sin\beta} + \frac{\partial\omega_0}{\partial c}c \\
\bar{f} &= -\frac{\partial\omega_0}{\partial\alpha}\frac{\cos\gamma}{\sin\beta} + \frac{\partial\omega_0}{\partial\beta}\frac{1}{\sin\alpha} \\
\bar{g} &= -\frac{\partial\omega_1}{\partial\alpha}\frac{\cos\beta}{\sin\gamma} - \frac{\partial\omega_1}{\partial\beta}\frac{\sin\beta\cos\gamma}{\sin\alpha\sin\gamma} \\
\bar{h} &= -\frac{\partial\omega_1}{\partial\alpha}\frac{\cos\gamma}{\sin\gamma} + \frac{\partial\omega_1}{\partial\beta}\frac{\sin\beta}{\sin\alpha\sin\beta} + \frac{\partial\omega_1}{\partial b}b.
\end{aligned}$$

*$u_0, u_1, u_2$ represent the unit edge vector $e_{pq}, e_{pr}, e_{qr}$.*

Using the last lemma, we can compute the index of any discrete surface $M$ that are critical points of any geometric energy $E$, by evaluating the number of eigenvalues of $H$. We have already proved that the local index of $M$ with respect to area functional and $E_2$ is always 0. This fact is not always true to geometric energies $E_3$ and $E_4$ given by

$$E_3(M) = \sum_{T\in M} R^2(T),$$

$$E_4(M) = \sum_{T\in M} R(T)\sqrt{A(T)},$$

where $R(T)$ is the radius of circumscribed circle and $A(T)$ is the triangle area $T$. In these cases, there are vertices in discrete surfaces having local index equal to $0, 1, 2$ or 3.

## 4.6 Maximum principle

In the smooth case, harmonic maps $u : S \subset \mathbb{R}^d \to \mathbb{R}^k$ solving an elliptic differential equation satisfy a maximum principle. This means, in any open domain $U \subset S$, the maximum and minimum of $u$ is attained at the boundary $\partial U$. In discrete case, a surface satisfies a maximum principle if any vertex is on the convex hull of its star.

In this section, we present our study of the maximum principle in triangulated surfaces that are critical points of geometric energies $E_1, E_2, E_3$. In each case we have a different result, so we will analyze the maximum principle for each geometric energy separately.

**Proposition 19** *(see (23)) Let $M$ be discrete minimal surface that is a critical point of the area. If the star of an interior vertex $p \in M$ consists of acute triangles then $p$ lies in the convex hull of its star.*

*Proof*:

Let $\{q_i; i = 1, \ldots, m\}$ be the vertices of the star of an interior vertex $p$. Since $M$ is a discrete minimal surface, all of its vertices it is given by

$$p = \frac{\sum_{i}^{m} (\cot \alpha_i + \cot \beta_i) q_i}{\sum_{i}^{m} \cot \alpha_i + \cot \beta_i}.$$

where $\alpha_i, \beta_i$ are angles opposite to edge $e_{pq_i}$.

If the angles of triangles $T = (p, q_i, q_{i+1})$ are acute, overall $i$, then

$$\cot \alpha_i + \cot \beta_i > 0.$$

Therefore, $p$ lies in the convex hull of $\{q_i; i = 1, \ldots, m\}$. ■

The previous property does not hold in a more general case. Figure 4.18 shows a counterexample of the maximum principle for discrete minimal surfaces, with the presence of obtuse triangles. In left image, we see the original model with 7 vertices and only one in the interior (the red small circles are the boundary vertices). The right image is the discrete minimal surface with fixed boundary. It is clear that the interior vertex is out of the convex hull.

The next proposition analyzes the maximum principle of critical points to geometric energy $E_2$.

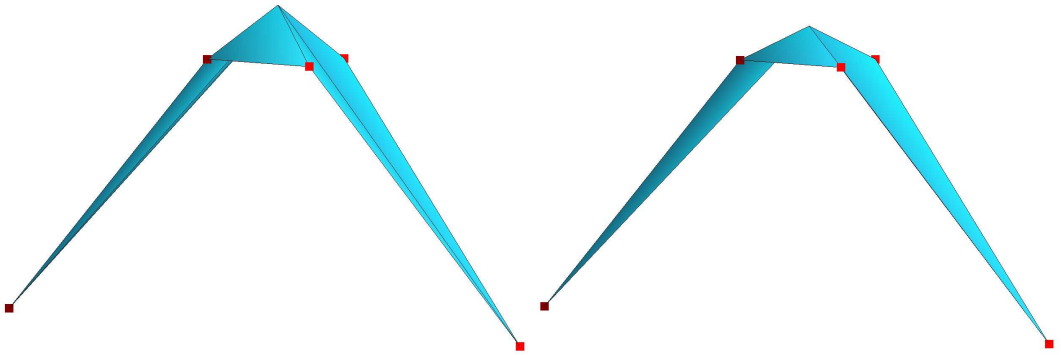

4.18(a): $M_0$ 4.18(b): $M_{47}$

Figure 4.18: *Counterexample to the maximum principle in discrete minimal surfaces.*

**Proposition 20** *Let $M$ be discrete surface that is a critical point to geometric energy $E_2$ and an interior vertex $p \in M$. Then $p$ is in the convex hull of its star.*

*Proof*:

Let $\{q_i; i = 1, \cdots, m\}$ be the vertices of the star of an interior vertex $p \in M$. Since $M$ is a critical point of $E_2$, $p$ is given by

$$p = \sum_{i=1}^{m} \frac{1}{m} q_i.$$

Therefore, $p$ is in the convex hull of $\{q_i; i = 1, \cdots, m\}$. ■

So, in the case of $E_2$, its critical points satisfy the maximum principle.

The next case is $E_3$. The maximum principle of critical points to geometric energy $E_3$ is analogous to the case $E_1$.

**Proposition 21** *Let $M$ be a critical point of $E_3$. If the star of an interior vertex $p \in M$ consists of acute triangles then $p$ lies in the convex hull of its star.*

*Proof*:

Let $\{q_i; i = 1, \cdots, m\}$ be the vertices of the star of an interior vertex $p$. Since $M$ is a critical point of $E_3$, all of its vertices are given by

$$p = \frac{\displaystyle\sum_{i}^{m} \left( \frac{\cot \alpha_i \cot \beta_i}{2 \sin^2 \gamma_i} + \frac{\cot \bar{\alpha}_i \cot \bar{\beta}_i}{2 \sin^2 \bar{\gamma}_i} \right) q_i}{\displaystyle\sum_{i}^{m} \frac{\cot \alpha_i \cot \beta_i}{2 \sin^2 \gamma_i} + \frac{\cot \bar{\alpha}_i \cot \bar{\beta}_i}{2 \sin^2 \bar{\gamma}_i}}.$$

where $\gamma_i, \bar{\gamma}_i, \alpha_i, \bar{\alpha}_i, \beta_i, \bar{\beta}_i$ are angles in triangles adjacent to $e_{pq_i}$, such that $\gamma_i, \bar{\gamma}_i$ are angles opposite to edge $e_{pq_i}$, $\alpha_i, \bar{\alpha}_i$ are angles at $p$ and $\beta_i, \bar{\beta}_i$ are the angles at $q_i$.

If the angles of triangles $T = (p, q_i, q_{i+1})$ are acute, overall $i$, then

$$\frac{\cot \alpha_i \cot \beta_i}{2 \sin^2 \gamma_i} + \frac{\cot \bar{\alpha}_i \cot \bar{\beta}_i}{2 \sin^2 \bar{\gamma}_i} > 0.$$

Therefore, $p$ lies in the convex hull of $\{q_i; i = 1, \cdots, m\}$. ■

As in the area case, the maximum principle property does not hold in general cases to critical points of $E_3$. Figure 4.19 shows a counterexample to the general case, once again with the presence of the obtuse angles. The left image is the original model with 4 points in a plane having only one interior point. The right image shows a critical point of $E_3$, where the interior point does not lie in the convex hull of its neighbors (represented by small red square).

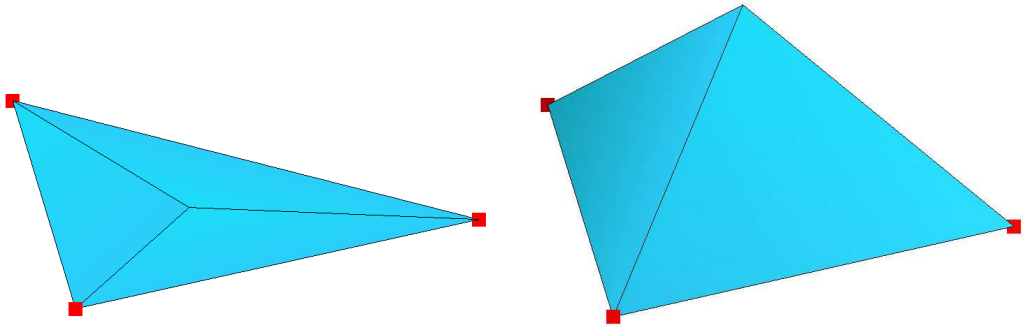

4.19(a): $M_0$ 4.19(b): $M_{282}$

Figure 4.19: *Counterexample to the maximum principle in critical points of* $E_3$.

Note also that the counterexample to the maximum principle for discrete minimal surfaces in general, presented in Figure 4.18, is not a counterexample to the maximum principle for critical points of the $E_3$. In Figure 4.20 we can see the minimization of $E_3$ over the same model of the Figure 4.18. In this case, the interior point of the final surface lies in the convex hull of its neighbors.

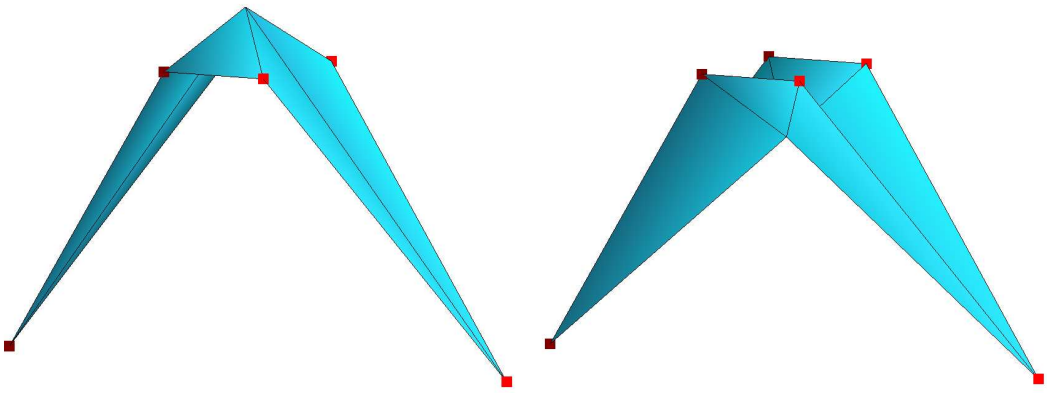

4.20(a): $M_0$ 4.20(b): $M_{40}$

Figure 4.20: *Example to the maximum principle in critical points of* $E_3$.

## 4.7 Homogeneous energies of degree 2

In this section, we show a simple relation between additive locally supported geometric energies defined on triangulated surfaces and area of the surfaces.

We recall that a function $f : \mathbb{R}^d \longrightarrow \mathbb{R}$ is called *homogeneous of degree m* if:

$$f(tp) = t^m f(p)$$

where $t \in \mathbb{R}$ and $p \in \mathbb{R}^d$.

We can consider geometric energies $E$ defined on triangulated surfaces $M$ as functions such that

$$E : \mathbb{R}^{3n} \longrightarrow \mathbb{R}$$

where $n$ is the number of the vertices of $M$. In this sense, we have the following lemma:

**Lemma 22** *The geometric energy $E$ is homogeneous of degree 2, if and only if, it can be written in the form:*

$$E(M) = \sum_{T \in M} f(\alpha, \beta) l^2,$$

*where $f$ is a real function of the angles $\alpha, \beta$ of the triangle $T$ in M and $l$ is one of its sides.*

*Proof*:

A geometric energy $E$ homogeneous of degree 2 certainly can be written as

$$E(M) = \sum_{T \in M} f(\alpha, \beta, l) l^2,$$

where $f$ is a real function of the triangle $T$ defined on its angles and side. In this case, $f$ must be homogeneous of degree $0$, i.e.,

$$f(\alpha, \beta, tl) = f(\alpha, \beta, l),$$

for $t \in \mathbb{R}$. This fact implies that

$$f(\alpha, \beta, l) = f(\alpha, \beta),$$

and we get the desired equation. ■

**Theorem 23** *Let $E$ be a geometric energy homogeneous of degree $2$ defined on a triangulated compact surface $M$ as*

$$E(M) = \sum_{T \in M} f(\alpha, \beta) l^2,$$

*where $f$ is a real function of $\alpha, \beta$, that are angles of the triangle $T$, and $l$ is one of its sides. If there exists a real number $c > 0$ such that*

$$f(\alpha, \beta) > 0$$

*in all triangles $T$ in $M$, when*

$$c \leq \theta \leq \pi - c$$

*for all angles $\theta$ of the triangles $T \in M$, then there exists $k, K > 0$ such that*

$$kArea(M) \leq E(M) \leq KArea(M).$$



*Proof*:

Considering a triangle $T$ as in Figure 4.16, we have

$$\begin{aligned} E(M) &= \sum_{T \in M} f(T) \\ &= \sum_{T \in M} f(a, b, c) \\ &= \sum_{T \in M} F(\alpha, \beta) l^2 \end{aligned}$$

where $l \in \{a, b, c\}$, $F$ is homogeneous with degree $0$ and by hypothesis $F > 0$. If $c \leq \theta \leq \pi - c$, for all angles in $M$, then

$$s \leq F(\alpha, \beta) \leq S,$$

for some $s, S \in \mathbb{R}$. In this case, if

$$k = min_{[c,\pi-c],[c,\pi-c]} F(\alpha, \beta)$$

$$K = max_{[c,\pi-c],[c,\pi-c]} F(\alpha, \beta),$$

we get the desired. ■

With this theorem, we conclude that any additive locally supported geometric energy homogeneous of degree $2$ of triangulated surfaces $M$ approximates the area of $M$ up to some multiplicative constants. This fact justifies the results obtained by minimization procedure of $E_3$, similar to discrete minimal surfaces.

# 5
# Discrete Willmore energies

In Chapter 4 we have studied additive locally supported geometric energies. Now we continue our study of geometric energies, by considering discrete Willmore energies. This energy captures the deviation of a surface from local spherecity, and it is used in many areas, as geometric and physical modeling.

Bobenko introduced the discrete version of Willmore energy studied here in (1), and it satisfies analogous discrete properties of the smooth case. We also introduce an alternative discrete Willmore energy. Its formulation is very simple when compared to the energy defined by Bobenko, and it provides good results. Neither of them are locally supported.



## 5.1
## Willmore energy

Bobenko in (1) defined a discrete version to Willmore functional, that we shall describe in this section. Before we show the discrete formulation, let us recall some definition and properties of smooth case.

### 5.1.1
### Smooth Willmore energy

In this subsection, we recall some definitions and cite some properties of the smooth Willmore functional. For more details, we recommend (36).

In 1965 the German mathematician T.J.Willmore proposed to study the functional

$$\bar{E}_W(X) = \int_S H^2 dA,$$

on immersions $X : S \longrightarrow \mathbb{R}^3$, where $S$ is a compact surface, $H$ is the mean curvature of the immersion and $dA$ the area element from $S$.

Defining

$$E_W(X) = \int_S (H^2 - K) dA,$$

so, by the Gauss-Bonnet theorem,

$$E_W(X) = \bar{E}_W(X) - 2\pi\chi(S),$$

since,

$$\int_S K dA = 2\pi\chi(S),$$

where $\chi(S)$ represents the Euler characteristic of the surface $S$. Therefore, both functionals differ by a constant. Actually, the new functional $E_W$ has the advantage that its integrand is nonnegative and vanishes exactly at the umbilic points of the immersion $X$. Based on that, we have the following definition:

**Definition 24** *The Willmore energy of a surface $S \subset \mathbb{R}^3$ is given by:*

$$\begin{aligned} E_W(S) &= \int_S (H^2 - K) dA \\ &= \frac{1}{4}\int_S (k_1 - k_2)^2 dA \end{aligned} \tag{5-1}$$

*where $k_1, k_2$ denote the principal curvatures, $H = \frac{1}{2}(k_1 + k_2)$ and $K = k_1 k_2$ the Gaussian and mean curvatures, respectively.*

Observing Equation 5-1, we conclude that $E_W(S) \geq 0$ and $E_W(S) = 0$, if and only if, $S$ is a sphere.

In 1973, J.H. White proved that the 2-form $(H^2 - K)dA$ is invariant under conformal transformations of $S^3$. Therefore, the Willmore functional is a conformal invariant of a surface (see (35)).

### 5.1.2 Discrete Willmore energy

In this section, we consider the discrete version of Willmore energy defined in (1, 2).

**Definition 25** *The discrete Willmore energy of a vertex $p \in M$ is given by*

$$W_1(p) = -2\pi + \sum_{q \in N(p)} \beta(e_{pq}),$$

*where $\beta(e_{pq})$ is the angle between the circumscribed circles to $t_{pqr}$ and $t_{qps}$ adjacent to edge $e_{pq}$ (see Figure 5.1).*

*The discrete Willmore energy of $M$ is the sum over all vertices of $M$:*

$$\begin{aligned} W_1(M) &= \frac{1}{2}\sum_p W_1(p) \\ &= -n\pi + \sum_{e_{pq} \in Edges(M)} \beta(e_{pq}). \end{aligned}$$

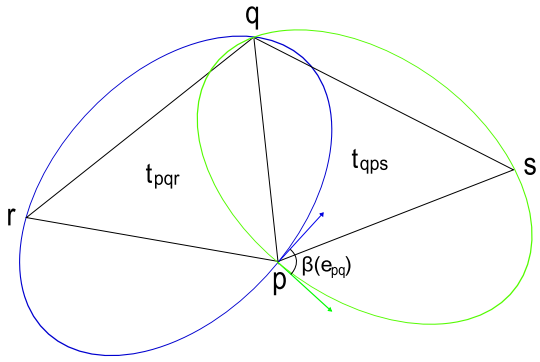


Figure 5.1: *Angle $\beta(e_{pq})$ between the circumscribed circles to triangles $t_{pqr}$ and $t_{qps}$.*

Obviously, $W_1$ is Mobius invariant since its definition is based on angles between circles, keeping an important property of the classical Willmore energy defined for smooth surfaces. Besides that, the definition above provides not only a discrete analogue of the Willmore energy, but it also approximates the smooth energy, as we can see in (2). One more analogous property is shown in the next theorem:

**Theorem 26** *The discrete Willmore energy of $M$ is nonnegative, i.e.,*

$$W_1(M) \geq 0.$$

*And, $W_1(M) = 0$ if, and only if, $M$ is (part of a) convex polyhedron inscribed in a sphere.*

The proof can be found in (1).

Numerically, to solve energy minimization problems, it is convenient to evaluate the explicit value of $W_1$ and its derivative, using only the vertices of the surface. For this propose, we begin showing how to compute the angle $\beta(e_{pq})$, between circumscribed circles of the triangles $t_{pqr}$ e $t_{qps}$, by the proposition:

**Proposition 27** *Consider two triangles $t_{pqr}$, with vertices $p, q, r$ and $t_{qps}$, with vertices $q, p, s$, adjacent to edge $e_{pq}$, as in Figure 5.1. The external angle $\beta(e_{pq}) \in [0, \pi]$ between $t_{pqr}$ and $t_{qps}$ is given by*

$$\cos\beta(e_{pq}) = \frac{< a, c >< b, d > - < a, b >< c, d > - < b, c >< d, a >}{|a||b||c||d|}, \quad (5\text{-}2)$$

*where $<,>$ denotes the inner Euclidean product, and*

$$a = q - s, b = r - q$$

$$c = p - r, d = s - p.$$

This proof also can be found in (1).

We note that the angle $\beta(e_{pq})$ between the circumscribed circles to $t_{pqr}$ and $t_{qps}$ is equal to the angle $\beta(e_{qp})$. And changing the orientation of both circles, the angle $\beta(e_{pq})$ is preserved. This shows that the energy $W_1$ is well-defined for non-oriented surfaces as well. And if $\beta(e_{pq}) = \beta(s,q,r,p)$, then $\beta(e_{pq}) = \beta(s,q,r,p) = \beta(r,p,s,q) = \beta(e_{qp})$. In fact, $\cos\beta(e_{pq})(r,q,r,p)$ in terms of scalar products is invariant by cyclic permutations and reflections of its arguments. In particular, if we flip the edge $e_{pq}$ to $e_{rs}$, the cosine of the angle remains the same.

From the last proposition, a direct calculation provides the Willmore energy gradient. For this propose, we suppose that a surface $M$ has two adjacent triangles $t_{pqr}$ e $t_{qps}$. It is convenient to use the following notation:

$$\begin{aligned} A &= \frac{a}{|a|} = \frac{q-s}{|q-s|}, \\ B &= \frac{b}{|b|} = \frac{r-q}{|r-q|}, \\ C &= \frac{c}{|c|} = \frac{p-r}{|p-r|}, \\ D &= \frac{d}{|d|} = \frac{s-p}{|s-p|}, \\ \beta &= \beta(e_{pq}). \end{aligned}$$

It is proved in (2) that the Willmore energy gradient is given by:

$$\nabla_p W_1(M) = C_1(p-q) + C_2(p-r) + C_3(p-s) \tag{5-3}$$

where,

$$\begin{aligned} C_1 &= \frac{< A,C >}{|b||d|\sin\beta} + \frac{< D,A >}{|b||c|\sin\beta} + \frac{< B,D >}{|a||c|\sin\beta} + \frac{< B,C >}{|a||d|\sin\beta} \\ C_2 &= -\frac{< B,D >}{|a||c|\sin\beta} - \frac{< B,C >}{|a||d|\sin\beta} + \frac{\cos\beta}{|d|^2\sin\beta} - \frac{< A,B >}{|d||c|\sin\beta} \\ C_3 &= -\frac{< A,B >}{|d||c|\sin\beta} + \frac{\cos\beta}{|c|^2\sin\beta} - \frac{< A,C >}{|b||d|\sin\beta} - \frac{< D,A >}{|b||c|\sin\beta}. \end{aligned}$$

*Remark:* Considering a general surface with more than 2 triangles, the gradient of $W_1$ must be computed by

$$\nabla_p W_1(M) = \sum_{q\in N(p)} \nabla_p\beta(e_{pq}) + \sum_{t_{pqs}\in T(p)} \nabla_p\beta(e_{qs}),$$

where $\nabla_p\beta(e_{pq}), \nabla_p\beta(e_{qs})$ can be obtained by Equation 5-3 permuting the vertices, see Figure 5.2. It is clear that moving vertex $p$, then not only $\beta(e_{pq})$ will be

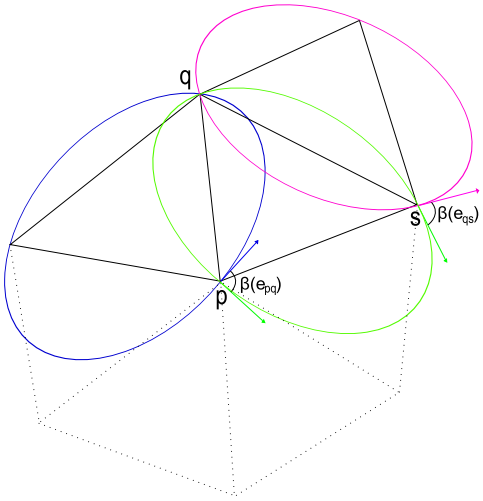


Figure 5.2: *Angles to gradient of* $W_1$.

moved, but $\beta(e_{qs})$ will also be moved. In contrast to the locally supported geometric energies gradient studied in last chapter, the Willmore energy gradient with respect to $p$ is evaluated by a sum over all edges of the two adjacent triangles to $p$.

A discrete surface $M$ is called the Willmore surface, if it is a critical point of the discrete Willmore energy, i.e., for all vertices $p \in M$ we have

$$\nabla_p W_1(M) = 0.$$

Let us show some Willmore surfaces obtained by minimization of $W_1$. The following results were obtained by steepest descent method described in section 2.1.

*Example 1:*

In the Figure 5.3 we have a minimization of Willmore energy $W_1$ over a cube with 110 vertices, Figure 5.3(a). The method parameters are: tolerance $\epsilon = 10^{-5}$ and the time step $dt = 10^{-4}$. This discrete surface converges quickly to a sphere, as we see in Figure 5.3(c).

*Example 2:*

In Figure 5.4, we show a Willmore surface obtained by the minimization of a triangulated surface with 32 vertices, Figure 5.4(a). The method parameters are: tolerance $\epsilon = 10^{-5}$ and the time step $dt = 10^{-2}$. The surface shown in Figure 5.4(c) is a Willmore surface.

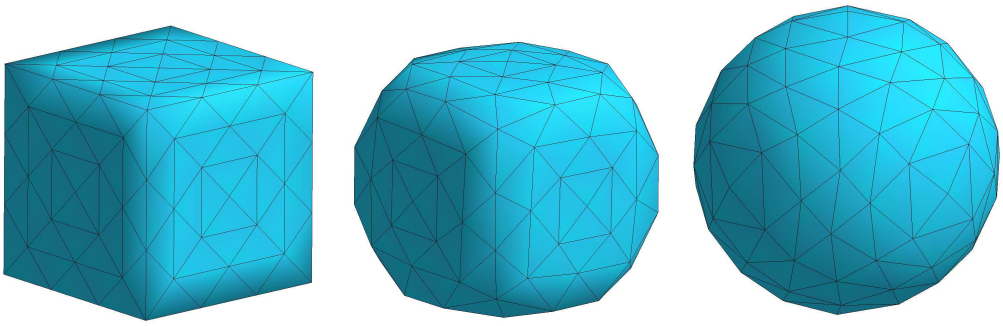

5.3(a): $M_0$ 5.3(b): $M_{300}$ 5.3(c): $M_{885}$

Figure 5.3: *Minimization of $W_1$ over a cube.*

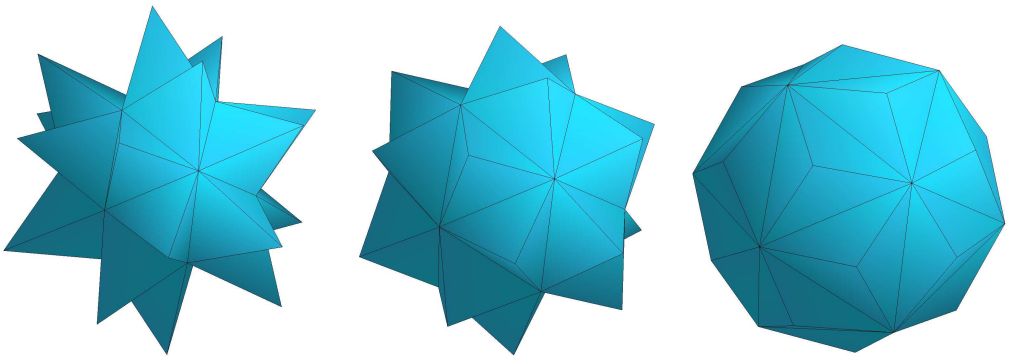

5.4(a): $M_0$ 5.4(b): $M_1$ 5.4(c): $M_{14}$

Figure 5.4: *Minimization of $W_1$ over a triangulated surface 5.4(a).*

## 5.2 Alternative discrete Willmore energy

In this section we present a new discrete energy that is an alternative discrete Willmore energy.

**Definition 28** *The energy $W_2$ of a discrete surface $M$ is given by*

$$W_2(M) = \sum_{e_{pq} \in Edges(M)} 4(1 - \cos\gamma(e_{pq})),$$

*such that, $\gamma(e_{pq})$ is the angle between normals of the triangles adjacent to $e_{pq}$ as we can see in Figure 5.5.*

Next we show that if the triangles do not degenerate, then

$$W_2(M) \approx \int_M H^2 dA,$$

where $H$ is the mean curvature of $M$.

Morvan et al. in (6) define

$$H(e_{pq})dA = \gamma(e_{pq})|e_{pq}|,$$

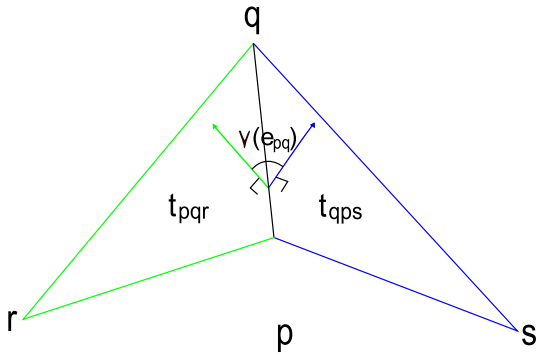


Figure 5.5: *Angle of* $W_2$.

where $\gamma(e_{pq})$ is the angle between normal of the triangles $t_{pqr}$ and $t_{qps}$ as in Figure 5.5, $|e_{pq}|$ the length of edge $e_{pq}$ and $dA$ is the area element. If the triangles do not degenerate, we can approximate the area of the triangles in $M$ by $\frac{|e_{pq}|^2}{2}$, i.e.,

$$dA = \frac{|e_{pq}|^2}{2},$$

what implies that

$$H(e_{pq})^2 dA = 2\gamma(e_{pq})^2.$$

Since

$$\cos\gamma(e_{pq}) \approx 1 - \frac{\gamma(e_{pq})^2}{2},$$

$W_2(M)$ is close to the Willmore energy.

**Corollary 29** *The alternative discrete Willmore energy of* $M$ *is nonnegative, i.e.,*

$$W_2(M) \geq 0.$$

*And,* $W_2(M) = 0$ *if, and only if,* $M$ *is on a plane.*

Note that this alternative Willmore energy $W_2$ is a conformal invariant, since its definition is based on angles. Besides that, it is not a locally supported energy.

In (1), Bobenko suggest to approximate the discrete Willmore energy $W_1$ by

$$E(M) = \sum_{e_{pq} \in Edges(M)} \frac{|e_{pq}|}{d_{pq}} \gamma^2(e_{pq}),$$

where $d_{pq}$ is the distance between the centers of the circumscribed circles to $t_{pqr}$ and $t_{qps}$, that is near to $W_2$. He also suggest that this approximation can be used for bending discrete surfaces, specially thin-shells that are thin flexible structures with a high ratio of width to thickness. In (13), Desbrun et al. used a similar energy to

$W_2$ to simulate thin shells

$$\bar{E}(M) = \sum_{e_{pq} \in Edges(M)} \frac{|e_{pq}|}{h_{pq}} \gamma^2(e_{pq}),$$

where $h_{pq}$ is a third of the mean of the heights of the triangles $t_{pqr}$ and $t_{qps}$. Note that, $W_2$ is a simpler way to define these two energies used to simulate thin shells, which motivate to study the applications of $W_2$ in the future.

We wish to compute the gradient of $W_2$, so it is convenient to compute $\cos\gamma(e_{pq})$ explicitly. For this propose, consider three triangles $t_{pqr}, t_{qps}, t_{rqt}$ in $M$, as in the Figure 5.6. Let $N_{pqr}, N_{qps}, N_{rqt}$ be the normals of the triangles $t_{pqr}, t_{qps}, t_{rqt}$, respectively. Let $\theta$ be the angle between $N_{pqr}$ and $N_{qps}$, and $\psi$ the angle between $N_{pqr}$ and $N_{rqt}$. So,

$$\cos\theta = \frac{< N_{pqr}, N_{qps} >}{|N_{pqr}||N_{qps}|}$$

$$\cos\psi = \frac{< N_{pqr}, N_{rqt} >}{|N_{pqr}||N_{rqt}|}.$$

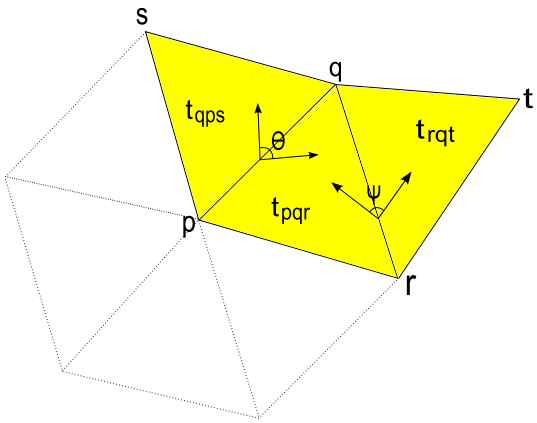


Figure 5.6: *Angles to gradient of* $W_2$.

Therefore,

$$\nabla_p W_2(M) = -4\Big( \sum_{q \in N(p)} \nabla_p \cos\theta + \sum_{t_{pqr} \in T(p)} \nabla_p \cos\psi \Big).$$

So, it follows that,

$$\begin{aligned}
\nabla_p W_2(M) \;=\; & -4\Big( \sum_{q \in N(p)} \frac{(r-q)\times N_{qps}}{|N_{pqr}||N_{qps}|} + \frac{N_{pqr}\times(s-q)}{|N_{pqr}||N_{qps}|} \\
& - \frac{< N_{pqr}, N_{qps} > N_{qps}\times(s-q)}{|N_{qps}|^3|N_{pqr}|} - \frac{< N_{pqr}, N_{qps} > (r-q)\times N_{pqr}}{|N_{qps}||N_{pqr}|^3} \\
& + \sum_{t_{pqr} \in T(p)} \frac{(r-q)\times N_{rqt}}{|N_{pqr}||N_{rqt}|} - \frac{< N_{pqr}, N_{rqt} > (r-q)\times N_{pqr}}{|N_{pqr}|^2|N_{rqt}|} \Big).
\end{aligned}$$

Although $W_2$ approximates the smooth Willmore energy, $W_2$ does not satisfy similar properties of $W_1$. For instance, the gradient of $W_2$ is not invariant under cyclic and reflections of its arguments. However, the formulation is very simple and the results are good visually.

Let us show some results obtained by implementation of the steepest descent method to minimization of $W_2$. The parameters of the method used in both examples are: tolerance $\epsilon = 10^{-5}$ and time step $dt = 10^{-3}$. We minimize over the same models of the previous chapter.

*Example 1:*

Figure 5.7 shows the minimization of $W_2$ over a cube with 110 vertices. And, as in the Willmore energy minimization, the cube becomes a sphere.

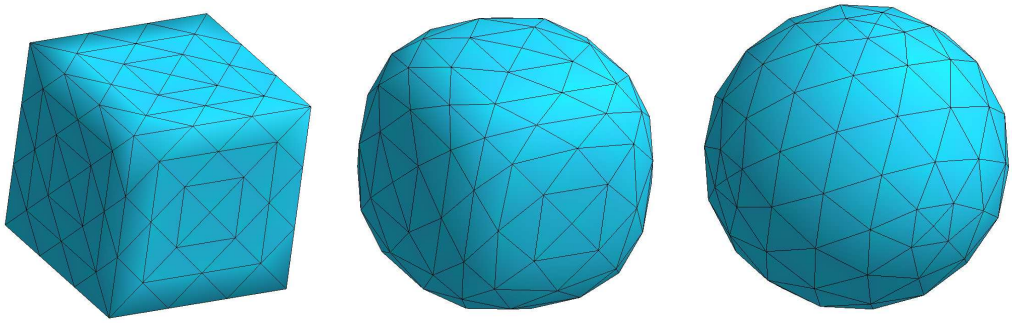

5.7(a): $M_0$ 5.7(b): $M_{200}$ 5.7(c): $M_{6646}$

Figure 5.7: *Minimization of $W_2$ over a cube.*

*Example 2:*

Figure 5.8 shows another example of the minimization of $W_2$, where we see a triangulated surfaces with 32 vertices converging to a sphere. The final surface, Figure 5.8(c), is close to final surface shown in Figure 5.4(c).

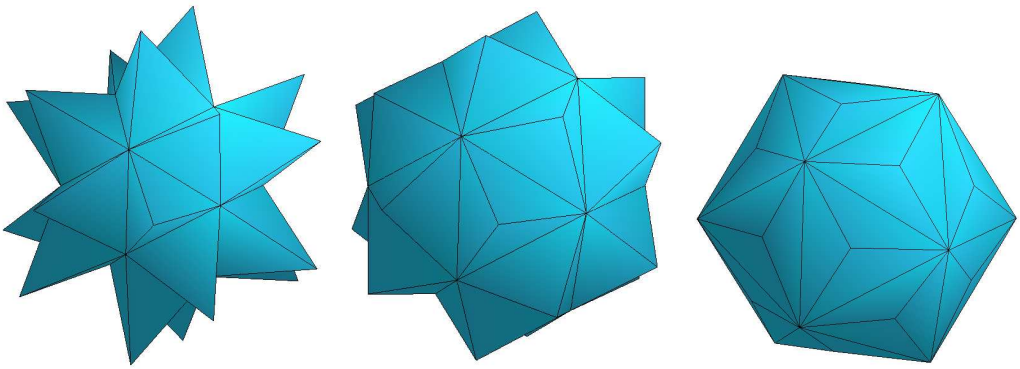

5.8(a): $M_0$ 5.8(b): $M_{17}$ 5.8(c): $M_{48}$

Figure 5.8: *Minimization of $W_2$ over a triangulated surface 5.8(a).*

# 6
# Conclusions

This thesis presented a study of geometric energies defined on triangulated surfaces.

An important known example of an additive locally supported geometric energy is the area functional. This energy was explored in different previous works and we shown some of its results. We constructed other examples of additive and locally supported geometric energy, called squared edges and circumscribed radius energy and we shown results obtained by the minimization of these energies.

Additive locally supported geometric energy is connected to discrete Laplacians. We proved that Laplacians that come from an geometric energy are symmetric. This is an interesting property, since the Laplacian matrix is symmetric, and therefore its eigenvalues are real and its eigenvectors are orthogonal. Besides that, we established conditions for a symmetric Laplacian to come from a geometric energy. These conditions must be satisfied by the triangles of the triangulated surface with its weighted edges given by the Laplacian.

We discussed the concept of index, defined to discrete minimal surfaces, i.e., we computed the number of negative eigenvalues of the Hessian of geometric energies. The eigenvectors associated to negative eigenvalues represent the directions of decreasing of the geometric energy. This is important to classify a critical point to geometric energy as a minimum or not.

We discussed the maximum principle to triangulated surfaces that are critical points of geometric energies. And we do not find a general result that works in all examples.

Besides that, we related homogeneous of degree 2 geometric energies with the area of the triangulated surface. Actually, we proved that any geometric energy that is a homogeneous function of degree 2 is an approximation of the area of the surface.

We have also shown a few results related to our study of additive geometric energies that do not satisfy the local support property. An important known example is the discrete Willmore energy. This discrete version approximates the smooth Willmore energy and satisfies conformal invariance. We have also proposed an alternative version to discrete Willmore energy.

## Bibliography


[1] BOBENKO, A. I. **A conformal energy for simplicial surfaces**. Combinatorial and Computational Geometry, 52:133–143, 2005.

[2] BOBENKO, A. I.; SCHRÖDER, P. **Discrete Willmore flow**. In: Desbrun, M.; Pottmann, H., editors, IN EUROGRAPHICS SYMPOSIUM ON GEOMETRY PROCESSING, p. 101–110, 2005.

[3] BOBENKO, A. I.; SPRINGBORN, B. A. **Minimal surfaces from circle patterns: geometry from combinatorics**. Annals of Mathematics, 164:231–264, 2006.

[4] BRAKKE, K. A. **The surface evolver**. Experimental Mathematics, 1(2):141–165, 1992.

[5] CALABI, E.; OLVER, P. J.; SHAKIBAN, C.; TANNENBAUM, A. ; HAKER, S. **Differential and numerically invariant signature curves applied to object recognition**. Int. J. Comput. Vision, 26(2):107–135, 1998.

[6] COHEN-STEINER, D.; MORVAN, J.-M. **Restricted Delaunay triangulations and normal cycle**. In: SCG '03: PROCEEDINGS OF THE NINETEENTH ANNUAL SYMPOSIUM ON COMPUTATIONAL GEOMETRY, p. 312–321, New York, NY, USA, 2003. ACM.

[7] CONCUS, P. **Numerical solution of the minimal surface equation**. Mathematics of Computation, 21:340–350, 1967.

[8] DESBRUN, M.; MEYER, M.; SCHRÖDER, P. ; BARR, A. **Implicit fairing of irregular meshes using diffusion and curvature flow**. In: SIGGRAPH '99: PROCEEDINGS OF THE 26TH ANNUAL CONFERENCE ON COMPUTER GRAPHICS AND INTERACTIVE TECHNIQUES, p. 317–324, New York, NY, USA, August 1999. ACM Press/Addison-Wesley Publishing Co.

[9] DO CARMO, M. P. **Geometria diferencial de curvas e superfícies**. SBM, Rio de Janeiro, 2 edition, 2006.

[10] DZIUK, G. **An algorithm for evolutionary surfaces**. Numerische Mathematik, 58(1):603–611, 1991.

[11] FLOATER, M. S. **Mean value coordinates**. Comput. Aided Geom. Des., 20(1):19–27, 2003.

[12] GOLUB, G. H.; LOAN, C. F. V. **Matrix computations**. The Johns Hopkins University Press, October 1996.

[13] GRINSPUN, E.; HIRANI, A. N.; DESBRUN, M. ; SCHRÖDER, P. **Discrete shells**. In: 2003 ACM SIGGRAPH / EUROGRAPHICS SYMPOSIUM ON COMPUTER ANIMATION, p. 62–67, August 2003.

[14] ISENBURG, M.; GUMHOLD, S. ; GOTSMAN, C. **Connectivity shapes**. In: IN IEEE VISUALIZATION 2001 CONFERENCE PROCEEDINGS, p. 135–142, 2001.

[15] JR., W. L. W. **On discrete Dirichlet and Plateau problems**. Numerische Mathematik, 3(1):359–373, 61.

[16] KARNI, Z.; GOTSMAN, C. **Spectral compression of mesh geometry**. In: EWCG, p. 27–30, 2000.

[17] LIPMAN, Y.; SORKINE, O.; ALEXA, M.; COHEN-OR, D.; LEVIN, D.; RÖSSL, C. ; SEIDEL, H.-P. **Laplacian framework for interactive mesh editing**. International Journal of Shape Modeling (IJSM), 11(1):43–61, 2005.

[18] MEYER, M.; DESBRUN, M.; SCHRÖDER, P. ; BARR, A. **Discrete differential–geometry operators for triangulated 2–manifolds**. In: Hege, H.-C.; Polthier, K., editors, MATHEMATICAL VISUALIZATION III, p. 35–57. Springer, Berlin, 2002.

[19] NEALEN, A.; IGARASHI, T.; SORKINE, O. ; ALEXA, M. **Laplacian mesh optimization**. In: PROCEEDINGS OF ACM GRAPHITE, p. 381–389, 2006.

[20] NEALEN, A.; IGARASHI, T.; SORKINE, O. ; ALEXA, M. **FiberMesh: designing freeform surfaces with 3D curves**. ACM Transactions on Graphics (Proceedings of ACM SIGGRAPH), 26(3):article no. 41, 2007.

[21] PINKALL, U.; POLTHIER, K. **Computing discrete minimal surfaces and their conjugates**. Experimental Mathematics, 2:15–36, 1993.

[22] POLTHIER, K. **Computational aspects of discrete minimal surfaces**. In: Hoffman, D., editor, PROCEEDINGS OF CLAY MATHEMATICS INSTITUTE SUMMER SCHOOL ON HARMONIC ANALYSIS, volume 2, p. 65 –111, 2004.

[23] POLTHIER, K.; ROSSMAN, W. **Discrete constant mean curvature surfaces and their index**. In: VISUALIZATION AND MATHEMATICS, p. 47–77. Springer Verlag, 1997.

[24] POLTHIER, K.; ROSSMAN, W. **Discrete catenoid**. Eletronic Geometry Models, 2000. http://www.eg-models.de/2000.05.002/.

[25] POLTHIER, K.; ROSSMAN, W. **Discrete minimal helicoid**. Eletronic Geometry Models, 2001. http://www.eg-models.de/2001.01.046/.

[26] SHARF, A.; LEWINER, T.; SHAMIR, A.; KOBBELT, L. ; COHEN-OR, D. **Competing fronts for coarse–to–fine surface reconstruction**. In: EUROGRAPHICS, p. 389–398, Vienna, september 2006.

[27] SORKINE, O. **Laplacian mesh processing**. PhD thesis, School of Computer Science, Tel Aviv University, 2006.

[28] SORKINE, O.; COHEN-OR, D. **Least-squares meshes**. In: PROCEEDINGS OF SHAPE MODELING INTERNATIONAL, p. 191–199. IEEE Computer Society Press, 2004.

[29] SORKINE, O.; COHEN-OR, D.; IRONY, D. ; TOLEDO, S. **Geometry-aware bases for shape approximation**. IEEE Transactions on Visualization and Computer Graphics, 11(2):171–180, 2005.

[30] SORKINE, O.; COHEN-OR, D. ; TOLEDO, S. **High-pass quantization for mesh encoding**. In: PROCEEDINGS OF THE EUROGRAPHICS/ACM SIGGRAPH SYMPOSIUM ON GEOMETRY PROCESSING, p. 42–51, Aachen, Germany, 2003. Eurographics Association.

[31] SULLIVAN, J. M. **A crystalline approximation theorem for hypersurfaces**. PhD thesis, Geometry Center – Princeton University, 1990.

[32] TAUBIN, G. **A signal processing approach to fair surface design**. In: SIGGRAPH '95: PROCEEDINGS OF THE 22ND ANNUAL CONFERENCE ON COMPUTER GRAPHICS AND INTERACTIVE TECHNIQUES, p. 351–358, New York, NY, USA, 1995. ACM.

[33] WACHSPRESS, E. L. **A Rational finite element basis**. Academic Press, 1975.

[34] WARDETZKY, M.; MATHUR, S.; KÄLBERER, F. ; GRINSPUN, E. **Discrete Laplace operators: no free lunch**. In: SGP '07: PROCEEDINGS OF THE FIFTH EUROGRAPHICS SYMPOSIUM ON GEOMETRY PROCESSING, p. 33–37, Aire-la-Ville, Switzerland, 2007. Eurographics Association.

[35] WHITE, J. **A global invariant of conformal mappings in spaces**. In: PROCEEDINGS AMERICAN MATHEMATICAL SOCIETY, volume 38, p. 162–164. American Mathematical Society, 1971.

[36] WILLMORE, T. J. **Riemannian geometry**. Oxford University Press, 1996.

[37] ZHANG, H. **Discrete combinatorial laplacian operators for digital geometry processing**. In: PROC. OF SIAM CONFERENCE ON GEOMETRIC DESIGN AND COMPUTING, p. 575–592. Nashboro Press, 2004.

# Livros Grátis

( http://www.livrosgratis.com.br )

Milhares de Livros para Download:

Baixar livros de Literatura
Baixar livros de Literatura de Cordel
Baixar livros de Literatura Infantil
Baixar livros de Matemática
Baixar livros de Medicina
Baixar livros de Medicina Veterinária
Baixar livros de Meio Ambiente
Baixar livros de Meteorologia
Baixar Monografias e TCC
Baixar livros Multidisciplinar
Baixar livros de Música
Baixar livros de Psicologia
Baixar livros de Química
Baixar livros de Saúde Coletiva
Baixar livros de Serviço Social
Baixar livros de Sociologia
Baixar livros de Teologia
Baixar livros de Trabalho
Baixar livros de Turismo